Atomic clocks and frequency transfer

Helen Margolis

Winter College on Optics
ICTP, Trieste, Italy (16th February 2016)

Outline (Part 1)

Timekeeping today and tomorrow

- Introduction of atomic time
- Cs microwave atomic clocks
- Coordinated Universal Time (UTC)
- Rationale for moving to the optical domain

Optical atomic clocks

- Components of an optical atomic clock
- Trapped ion optical clocks
  - Basic principles
  - Systems studied and state of the art performance
  - Systematic frequency shifts
- Current status of optical clocks and prerequisites for a redefinition of the SI second

Timekeeping today and tomorrow

Greenwich Mean Time (GMT)

Royal Observatory, Greenwich

Established as the global standard in 1884

Referred to mean solar time at the prime meridian in Greenwich

1 second = 1 / 86 400 of the mean solar day

The problem with this definition

"Yet, after all, the dimensions of our earth and its time of rotation, though, relatively to our present means of comparison, very permanent, are not so by physical necessity.

The Earth might contract by cooling, or it might be enlarged by a layer of meteorites falling on it, or its rate of revolution might slowly slacken, and yet it would continue to be as much a planet as before."

James Clerk Maxwell,

1870 meeting of the British Association for the Advancement of Science

A better solution

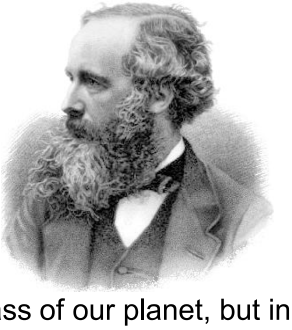

"But a molecule, say of hydrogen, if either its mass or its time of vibration were to be altered in the least, would no longer be a molecule of hydrogen.

If, then we wish to obtain standards of length, time, and mass which shall be absolutely permanent, we must seek them not in the dimensions, or the motion, or the mass of our planet, but in the wavelength, the period of vibration, and the absolute mass of these imperishable and unalterable and perfectly similar molecules."

James Clerk Maxwell,

1870 meeting of the British Association for the Advancement of Science

First caesium atomic clock

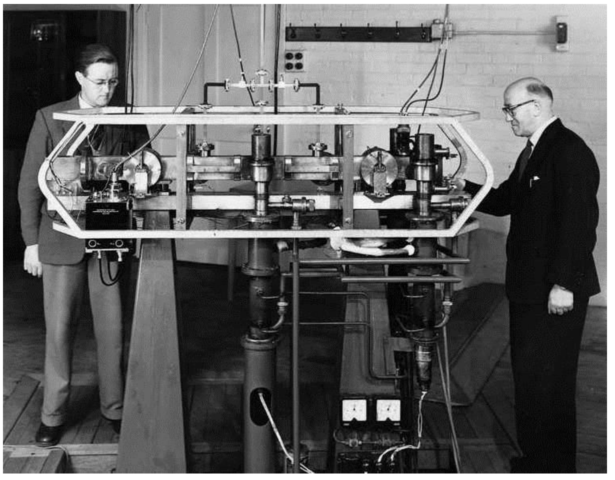

- Developed at NPL in 1955 by Louis Essen and Jack Parry
- Accurate to 1 part in 10^{10} (approximately 10 μs per day)

Introduction of atomic time

1958: International Atomic Time (TAI) began, following the development of further caesium clocks at NBS (USA) and ON (Switzerland)

1967: Caesium clock adopted as the basis for the international definition of time

> The second is the duration of 9 192 631 770 periods of the radiation corresponding to the transition between the two hyperfine levels of the ground state of the caesium-133 atom

Improvements in caesium atomic clocks

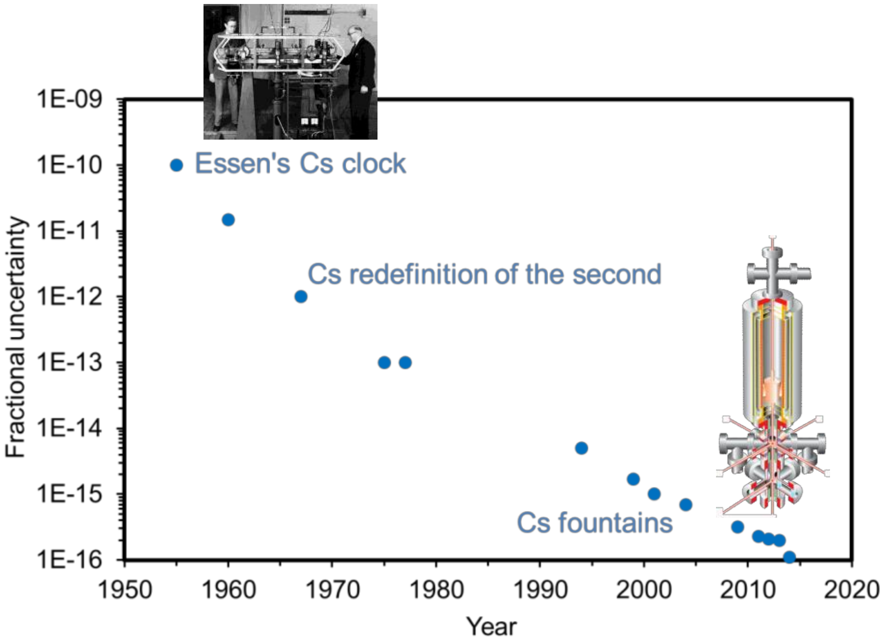

Two distinct tools

Timekeeping devices (true clocks)

- Absolute phase of the microwave signal is important

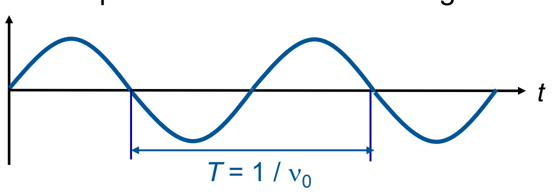

Primary frequency standards (not clocks!)

- Absolute phase of the microwave signal is not important

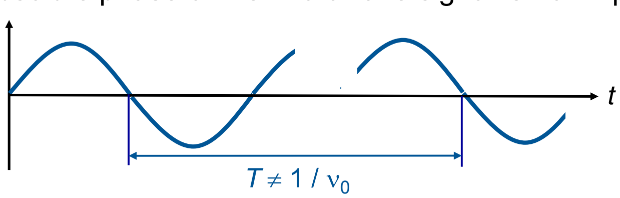

A frequency standard must work continuously to be a clock

Active & passive atomic frequency standards

All atomic frequency standards are based on the assumption that atomic transition frequencies are determined by fundamental constants

➡ They are the same for all atoms of a particular species

Two broad categories:

Active — Output signal derived directly from radiation emitted by an ensemble of atoms, e.g. active hydrogen maser

Passive — Atomic reference probed by radiation from an external oscillator

Passive atomic frequency standards

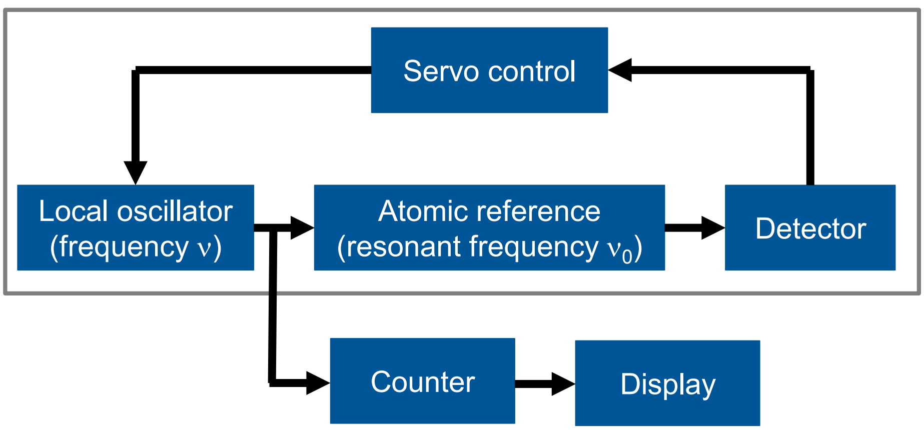

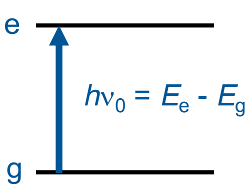

Linewidth of resonance $\Delta\nu \propto 1 / T$

T = interaction time (Rabi interrogation)

Ramsey spectroscopy

- To get a narrower line the interaction time must be increased
- Difficult to achieve high field uniformity over extended regions
- Use Ramsey's separated oscillatory field method

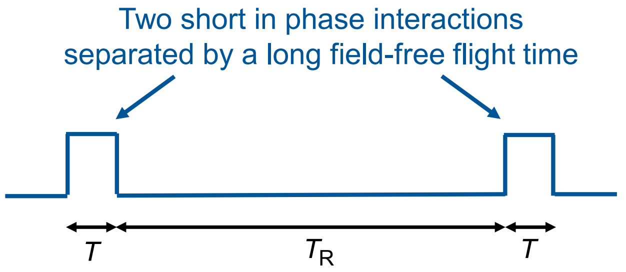

- Interference between atomic and electromagnetic phases
- Linewidth $\propto 1 / T_R$

Cs fountains

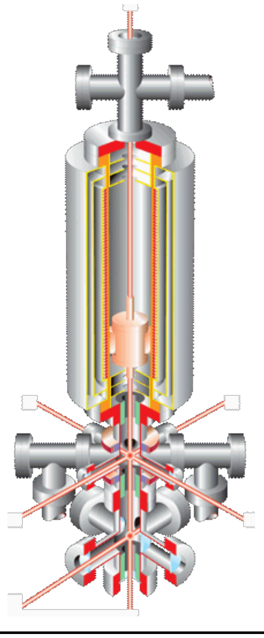

Use laser cooled atoms

T_R limited to ~1 s by the presence of gravity

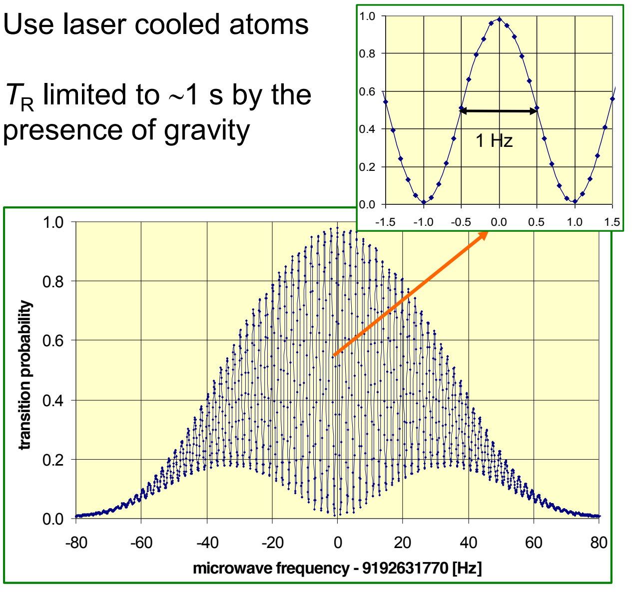

Cs fountain primary frequency standards

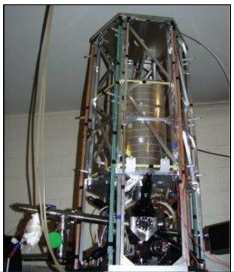

LNE-SYRTE FO2-Cs
Accuracy 2.1 parts in 10^{16}

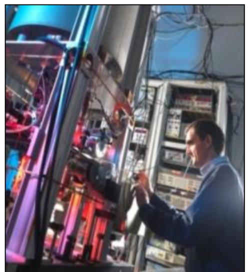

NPL-CsF2
Accuracy 2.0 parts in 10^{16}

PTB-CSF2
Accuracy 3.1 parts in 10^{16}

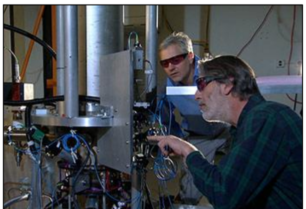

NIST-F2
Accuracy 1.1 parts in 10^{16}

INRIM ITCsF2
Accuracy 1.8 parts in 10^{16}

Coordinated Universal Time (UTC)

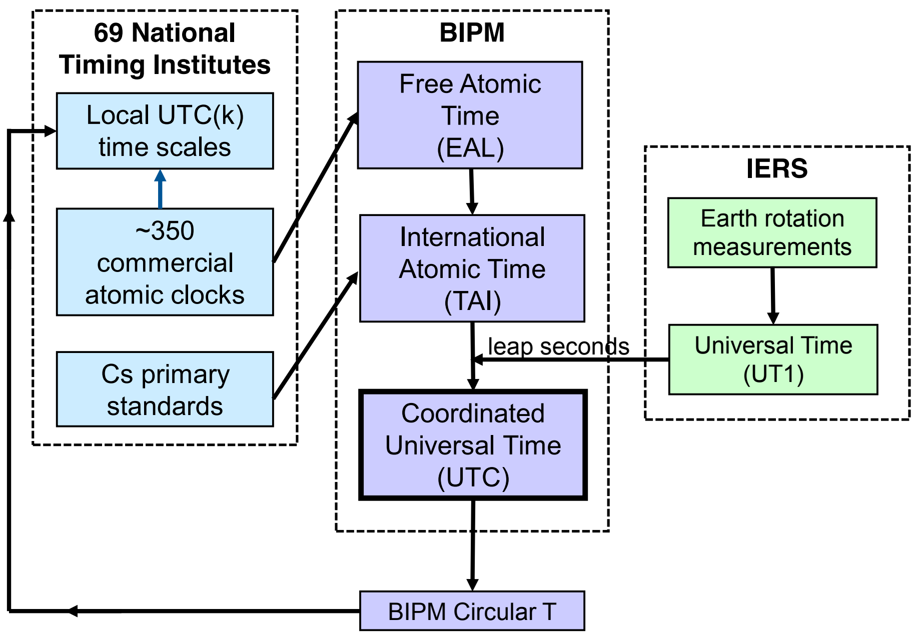

Timekeepers of the future

NPL | QMI

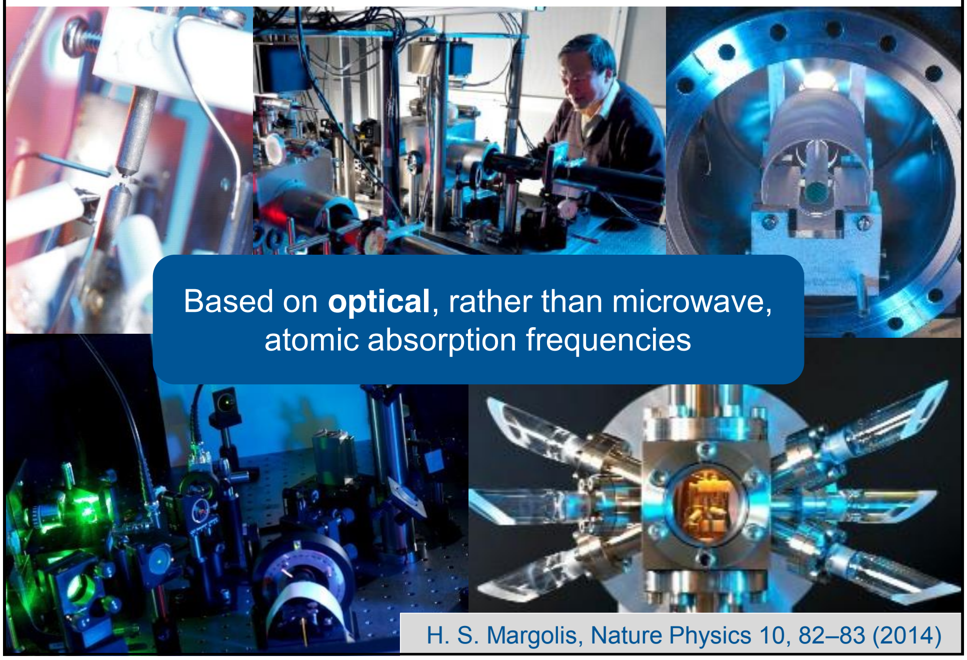

Performance of a frequency standard

NPL | QMI

(In)stability How much the frequency varies over some specified period of time (statistical uncertainties)

Reproducibility How well similar devices produce the same frequency

Accuracy How well the standard reproduces the internationally accepted time interval (i.e. the SI second)

but often…

How well the systematic frequency shifts can be characterised (estimated systematic uncertainty)

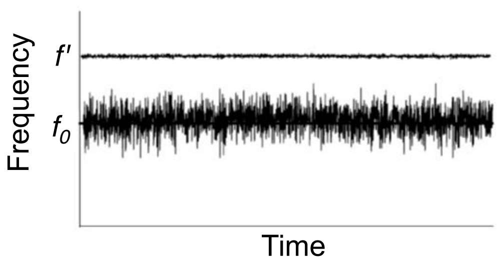

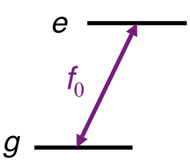

Allan variance and Allan deviation

Fractional frequency instability as a function of averaging time τ

$$\sigma_y^2(\tau) = \left\langle \frac{1}{2}(\bar{y}_{k-1} - \bar{y}_k)^2 \right\rangle \quad \text{where} \quad \bar{y}_k = \frac{1}{\tau}\int_{t_k}^{t_k+\tau} \frac{f(t) - f_0}{f_0}\, dt$$

$\sigma_y^2(\tau)$ = Allan variance

$\sigma_y(\tau)$ = Allan deviation

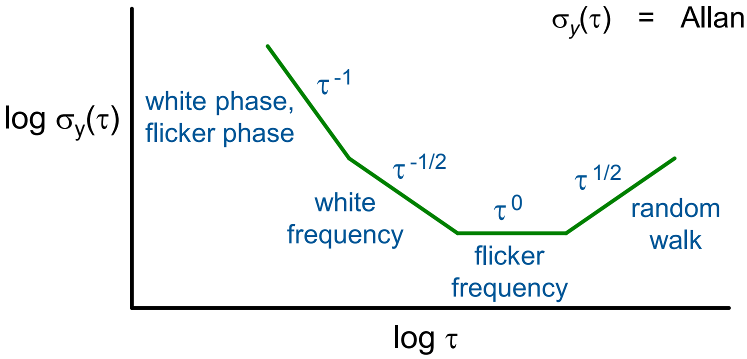

Advantage of optical clocks

Theoretically achievable fractional frequency instability:

$$\sigma_y(\tau) = \frac{\eta}{Q\,(S/N)}\,\tau^{-1/2}$$

$Q = \dfrac{f_0}{\Delta f}$ = line quality factor

(S/N) = signal-to-noise ratio for 1 Hz detection bandwidth

η ~ 1 (depends on shape of resonance and method used to determine f_0)

τ = averaging time in seconds

Advantage of optical atomic clocks

Optical clocks:

- Based on “forbidden” optical transitions in ions or atoms
- Natural linewidth Δf ~ 1 Hz (or less)
- Frequencies f_0 ~ 10^{15} Hz
- Q-factor ~ 10^{15} (or even higher)

	Microwave	Optical
f_0	~ 10^{10} Hz	~ 10^{15} Hz
Δf	~ 1 Hz	~ 1 Hz

5 orders of magnitude improvement in stability (in principle)

Optical atomic clocks

Components of an optical clock

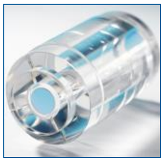

+

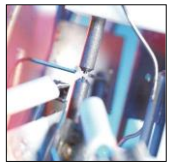

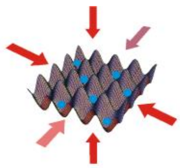

+

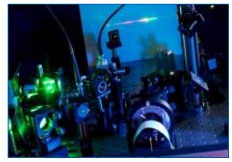

Oscillator
(Ultra-stable laser)

Reference
(narrow optical transition
in an ion or atom)

Counter
(Femtosecond comb)

Ultra-stable probe laser

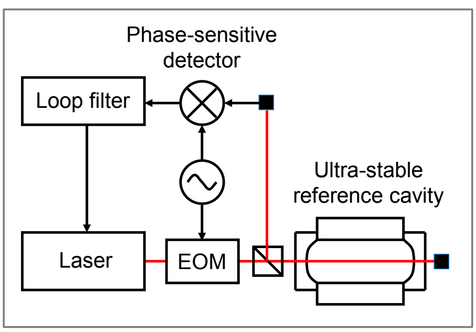

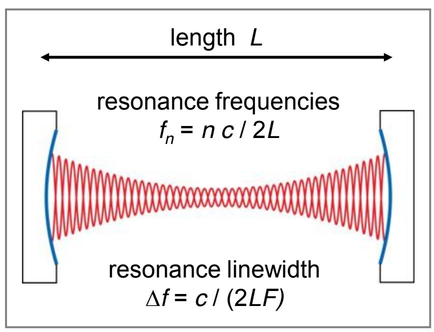

Drever *et al.*, Appl. Phys. B 31, 97 (1983)

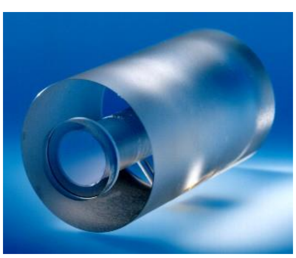

- High reflectivity mirrors contacted to ultra-low-expansion (ULE) glass spacer
- Optical finesse $F \sim 200{,}000$
- Temperature control to ± 1 mK
- Isolation from acoustic and seismic noise

Ultra-stable probe laser

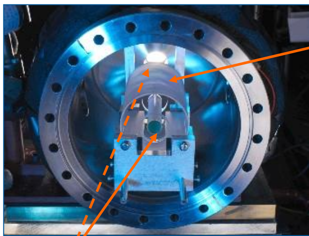

ULE glass spacer

- Length 10 cm
- Operated at temperature where coefficient of thermal expansion is zero
- Vibration-insensitive design

Optically contacted mirrors reflectivity > 99.998%

Acoustic isolation

Vibration-isolation platform

Laser linewidths ~ 1 Hz achieved

Vibration-insensitive cavity designs

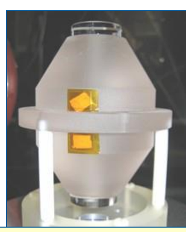

JILA vertical cavity mounted at midplane
Ludlow *et al.* Opt. Lett. 32, 641 (2007)

NPL cut-out cavity with 4-point support
Webster *et al.* PRA 75, 011801 (R) (2007)

NIST spherical cavity with 2-point support
Leibrandt *et al.*
Opt. Express 19, 3471 (2011)

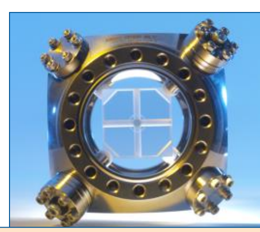

NPL cubic cavity with tetrahedral support
Webster and Gill, Opt. Lett. 36, 3572 (2011)

Thermal noise

$$\sigma_{\text{therm}} \propto \sqrt{\frac{T}{w_0 L^2}\left(\varphi_{\text{sub}} + k\frac{\varphi_{\text{coat}}}{w_0}\right)}$$

Theory: Numata *et al.*
PRL 93, 250602 (2004)

- Reduce mechanical loss φ_{sub} (e.g. by using fused silica substrates)

  Must compensate for mismatch of thermal expansion coefficient

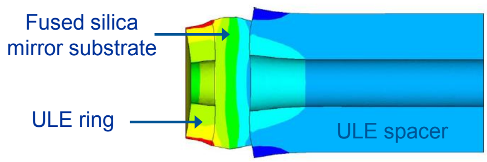

Legero *et al.*
J. Opt. Soc. Am. B 27, 914 (2010)

- Increase length L of spacer
- Increase 1/e beam radius w_0 on cavity mirrors
- Reduce temperature T of cavity

State-of-the-art performance

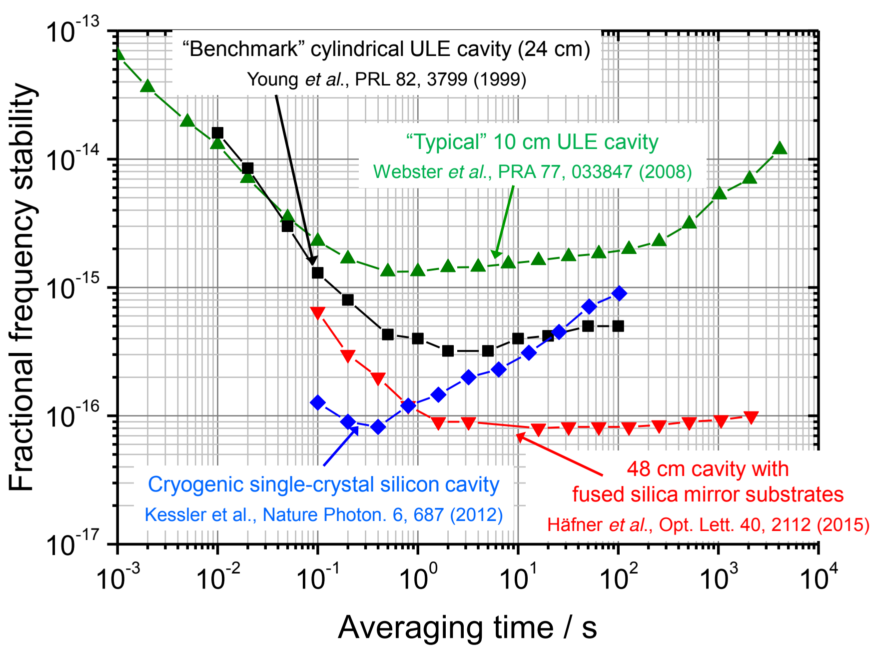

Candidates for the atomic reference

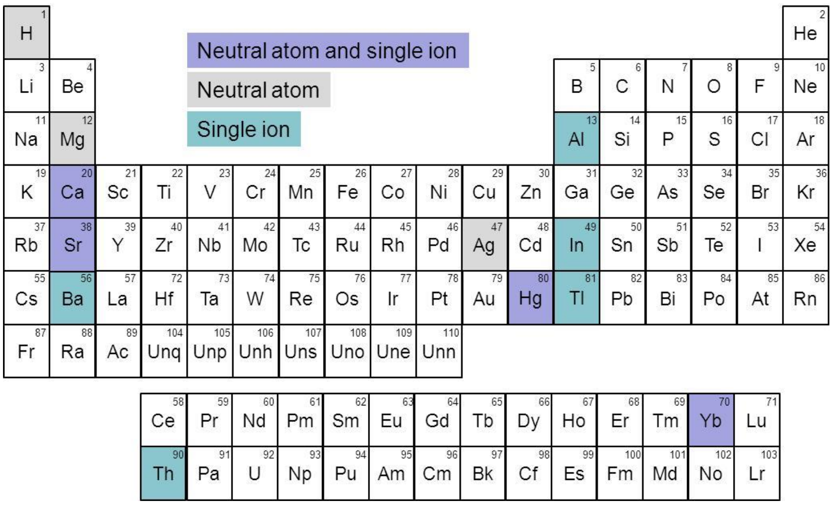

- Narrow optical transitions
- Insensitive to external perturbations
- Accessible clock transition wavelengths

Trapped ion optical clocks

- Based on "forbidden" (e.g. E2) transitions in single trapped ions ($Q \sim 10^{15}$)
- Long interrogation times possible

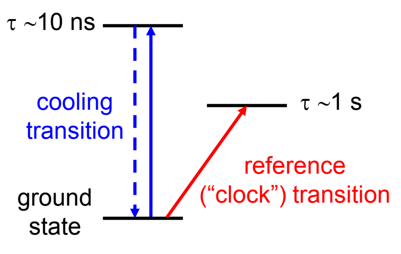

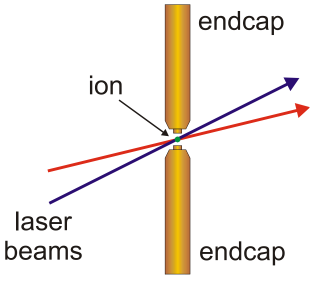

Low perturbation environment:

- No 1st-order Doppler shift
- Minimum 2nd-order Doppler shift
- Field perturbations minimised at trap centre
- Background collision rate low

Neutral atom lattice clocks

- $^1S_0 - {}^3P_0$ clock transitions (mHz natural linewidth)
- Atoms confined in an optical lattice
- *N* atoms, stability $\propto N^{1/2}$
- AC Stark shift eliminated by operating at "magic" wavelength

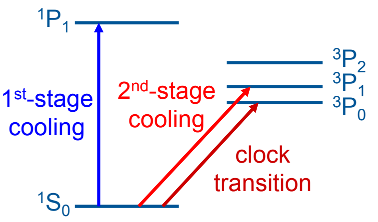

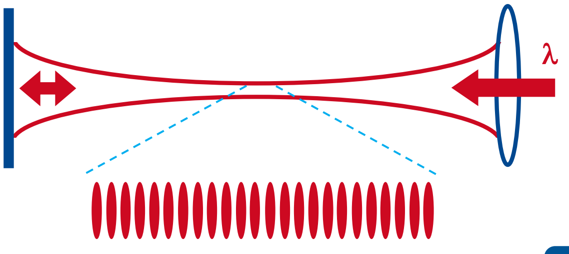

1D lattice, site spacing λ/2

Michał Zawada

Basic principles of trapped ion optical clocks

Principles of ion trapping

Quadrupole potential: $\phi(r, z, t) = A(t)\,(r^2 - 2z^2)$

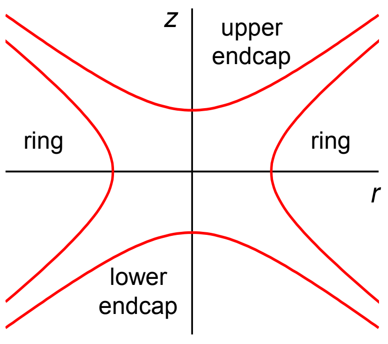

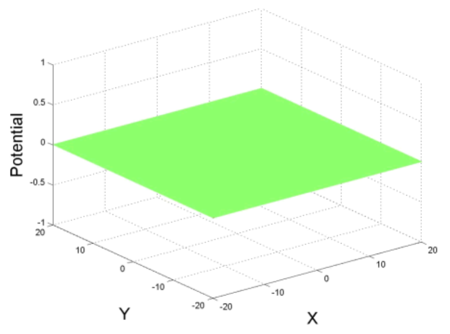

Radiofrequency voltage applied to ring electrode

→ ion trapped in time-averaged pseudopotential minimum

Motion of the trapped ion

Quadrupole potential: $\phi(r,z,t) = (Q_{dc} + Q_{ac}\cos\Omega t)\,(r^2 - 2z^2)$

Matthieu equation for motion of ion (writing $\tau = \Omega t / 2$):

$$\frac{d^2}{d\tau^2}\begin{bmatrix} x \\ y \\ z \end{bmatrix} + (a + 2q\cos 2\tau)\begin{bmatrix} x \\ y \\ -2z \end{bmatrix} = 0$$

where $a = \dfrac{8eQ_{dc}}{m\Omega^2}$ and $q = \dfrac{4eQ_{ac}}{m\Omega^2}$

For stable solutions, ion motion can be separated into two parts:

Micromotion Driven oscillatory motion at frequency Ω (vanishes at trap centre)

Secular motion Slower motion associated with time-averaged confining potential (characteristic frequencies ω_r and ω_z)

Minimization of the micromotion

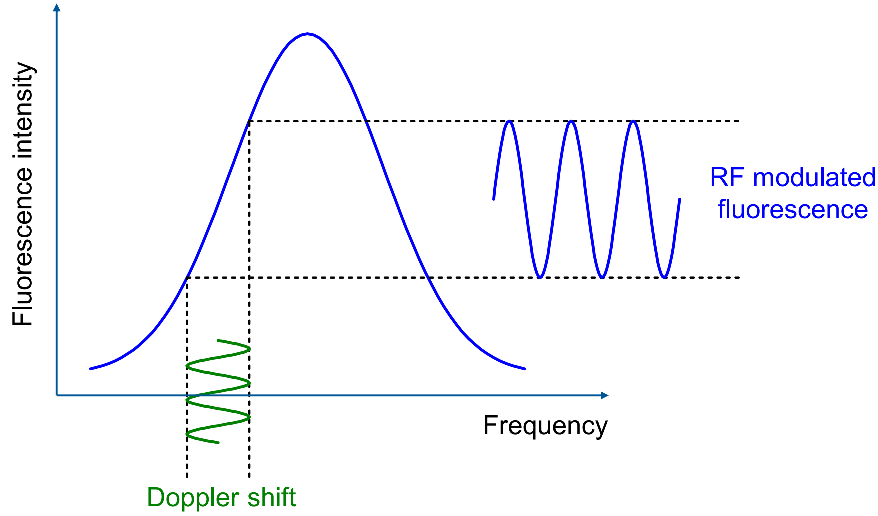

RF photon correlation technique:
Berkeland *et al.*, J. Appl. Phys. 83, 5025 (1998)

Ion traps for optical frequency standards

Ring traps

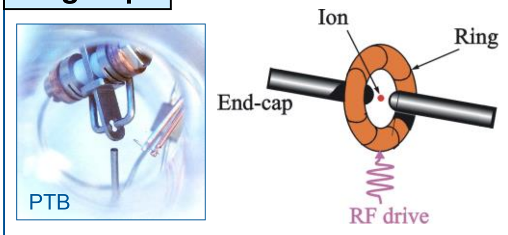

Endcap traps

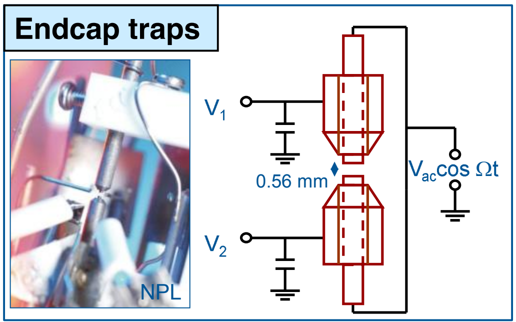

Linear traps

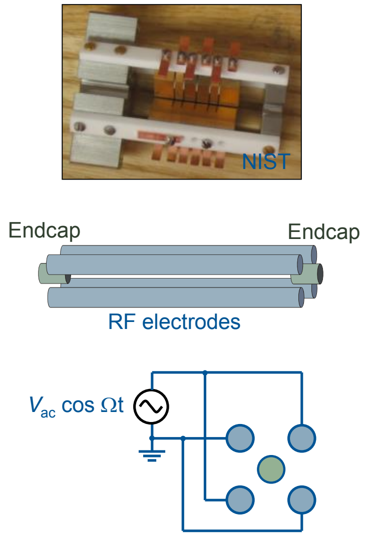

Electron shelving scheme

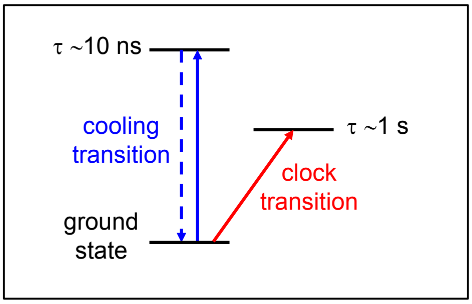

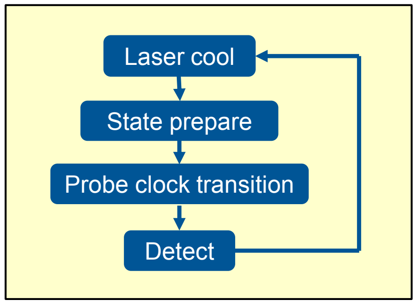

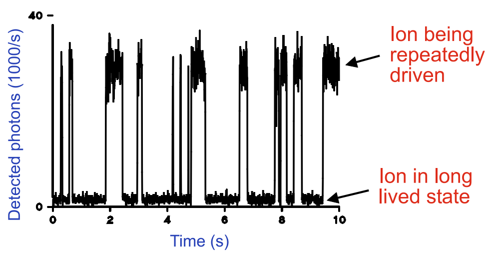

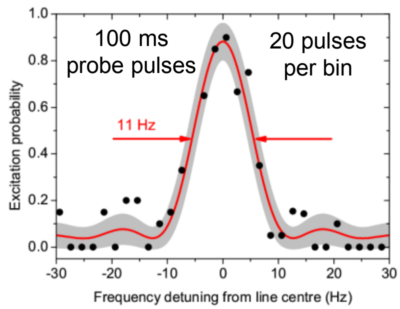

Laser stabilisation to the clock transition

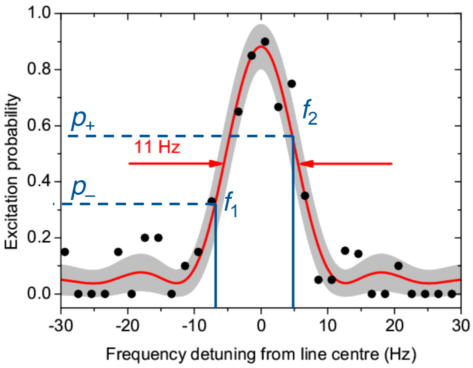

- Number of quantum jumps sampled at two frequencies f_1 and f_2
- Typically 20 interrogations each side of line centre

- Excitation probabilities used to produce error signal $e = \dfrac{p_+ - p_-}{p_+ + p_-}$
- Fed to doubly integrating servo to correct frequency of probe laser

![NPL | QMI logos]

Systems studied and state-of-the-art performance

Ion clocks: candidate systems (1)

Ions with alkali-like or quasi-alkali-like atomic structure

1 H																	2 He
3 Li	4 Be											5 B	6 C	7 N	8 O	9 F	10 Ne
11 Na	12 Mg											13 Al	14 Si	15 P	16 S	17 Cl	18 Ar
19 K	20 Ca	21 Sc	22 Ti	23 V	24 Cr	25 Mn	26 Fe	27 Co	28 Ni	29 Cu	30 Zn	31 Ga	32 Ge	33 As	34 Se	35 Br	36 Kr
37 Rb	38 Sr	39 Y	40 Zr	41 Nb	42 Mo	43 Tc	44 Ru	45 Rh	46 Pd	47 Ag	48 Cd	49 In	50 Sn	51 Sb	52 Te	53 I	54 Xe
55 Cs	56 Ba	57 La	72 Hf	73 Ta	74 W	75 Re	76 Os	77 Ir	78 Pt	79 Au	80 Hg	81 Tl	82 Pb	83 Bi	84 Po	85 At	86 Rn
87 Fr	88 Ra	89 Ac	104 Unq	105 Unp	106 Unh	107 Uns	108 Uno	109 Une	110 Unn								

58 Ce	59 Pr	60 Nd	61 Pm	62 Sm	63 Eu	64 Gd	65 Tb	66 Dy	67 Ho	68 Er	69 Tm	70 Yb	71 Lu
90 Th	91 Pa	92 U	93 Np	94 Pu	95 Am	96 Cm	97 Bk	98 Cf	99 Es	100 Fm	101 Md	102 No	103 Lr

Alkali-like systems

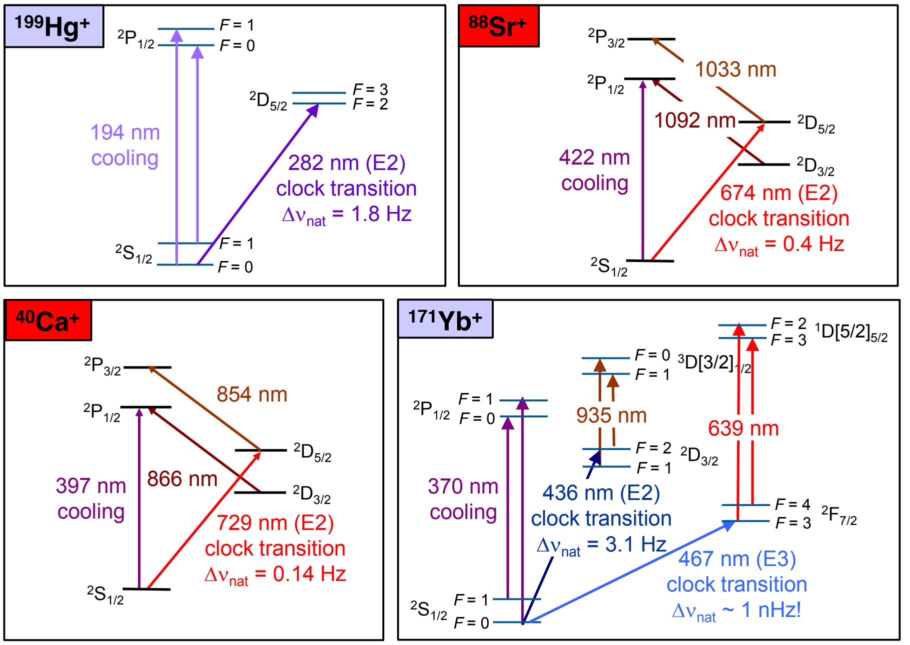

Ion clocks: candidate systems

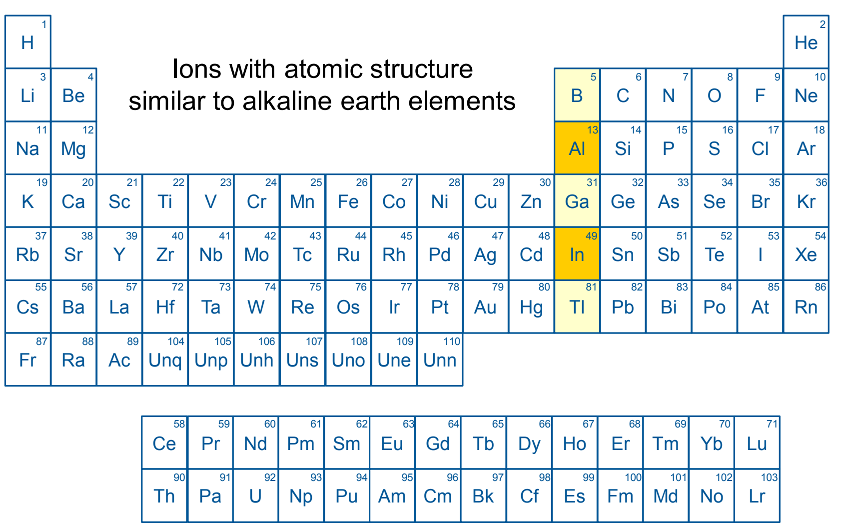

Alkaline-earth-like systems

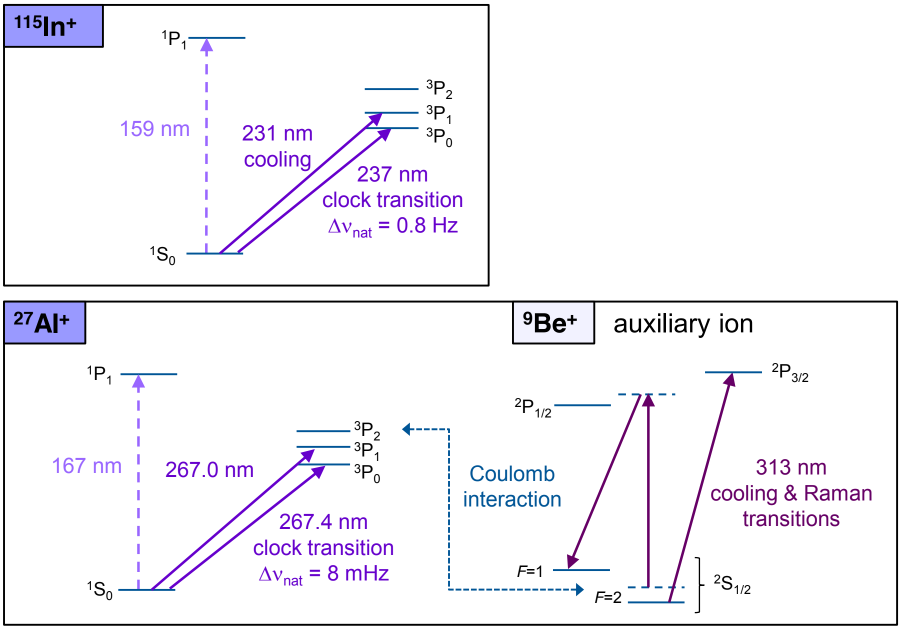

Cold ion *Q*-factors

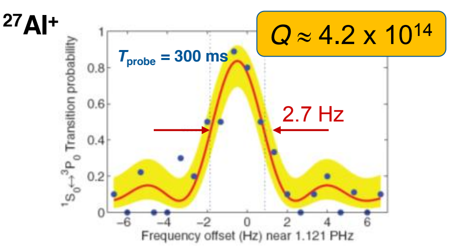

Chou *et al.*, Science 329, 1630 (2010)

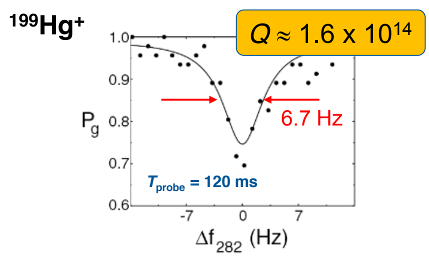

Rafac *et al.*, PRL 85, 2462 (2000)

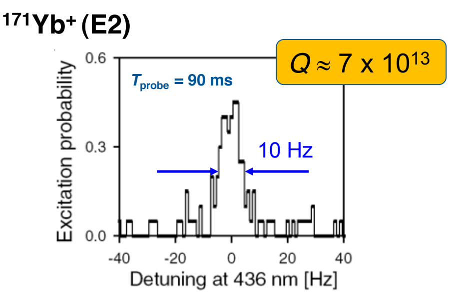

Peik *et al.*, PRL 93, 170801 (2004)

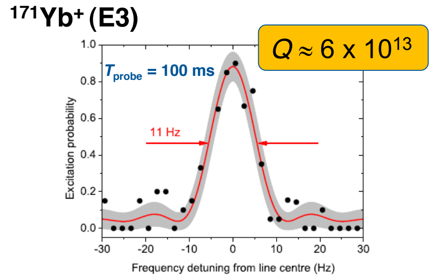

King *et al.*, New J. Phys. 14, 013045 (2012)

Measuring stability and reproducibility

Fractional instability $\sigma(\tau) = \frac{\Delta\nu}{\nu} \frac{\eta}{(S/N)} \tau^{-1/2}$

- Compare two independent optical frequency standards
- Measure $(\nu_1 - \nu_2)$ for a period of time, repeatedly.

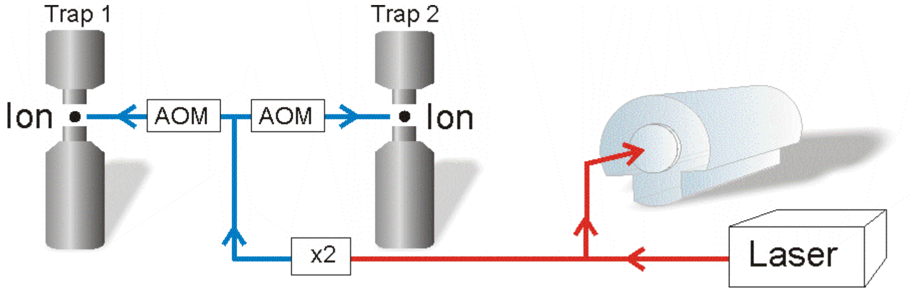

Stability and reproducibility

Comparison of two $^{27}Al^+$ standards at NIST

$^{27}Al^+$ / $^{9}Be^+$ u_B ~2.3×10^{-17}

$^{27}Al^+$ / $^{25}Mg^+$ u_B ~8.6×10^{-18}

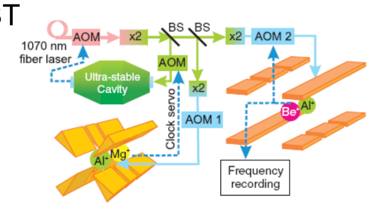

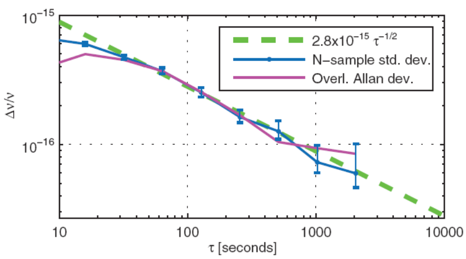

Fractional frequency instability
$2.8 \times 10^{-15}\ \tau^{-1/2}$

Fractional frequency difference
$-1.8\ (\pm 2.6) \times 10^{-17}$

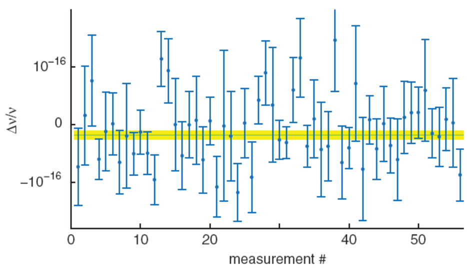

Chou *et al.*, PRL 104, 070802 (2010)

Other reproducibility tests

Comparison of two $^{88}Sr^+$ standards at NPL:

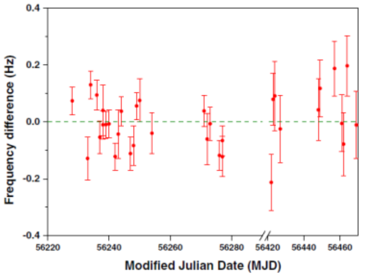

Fractional frequency difference
$0.9\ (\pm 4.0) \times 10^{-17}$

Barwood *et al.*,
PRA 89, 050501(R) (2014)

Comparison of two $^{40}Ca^+$ standards at WIPM:

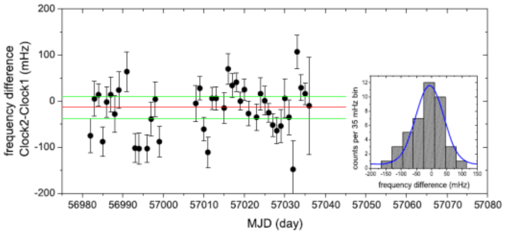

Fractional frequency difference
$3.2\ (\pm 5.5) \times 10^{-17}$

Huang *et al.*,
PRL 116, 013001 (2016)

Measuring the absolute frequency

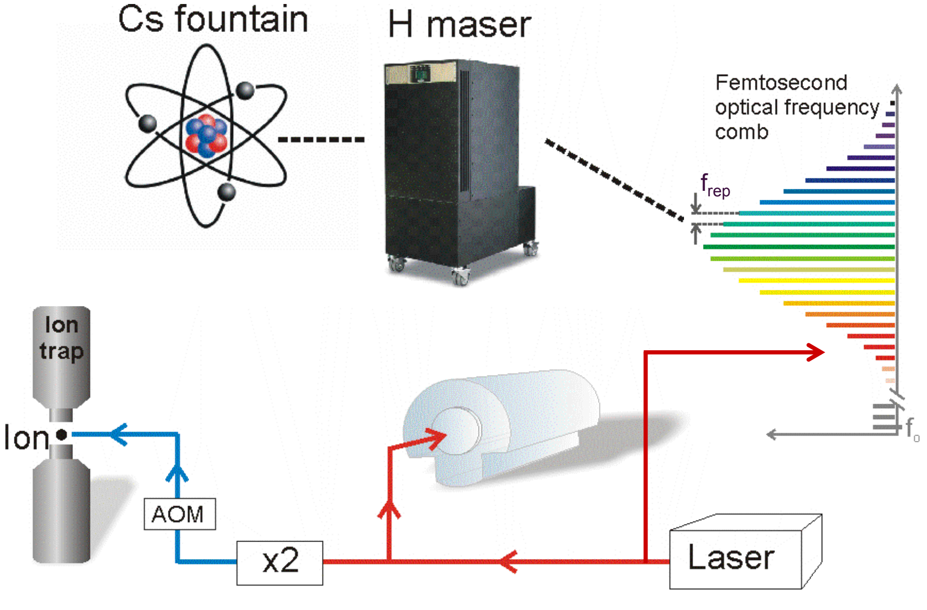

Absolute frequency measurements

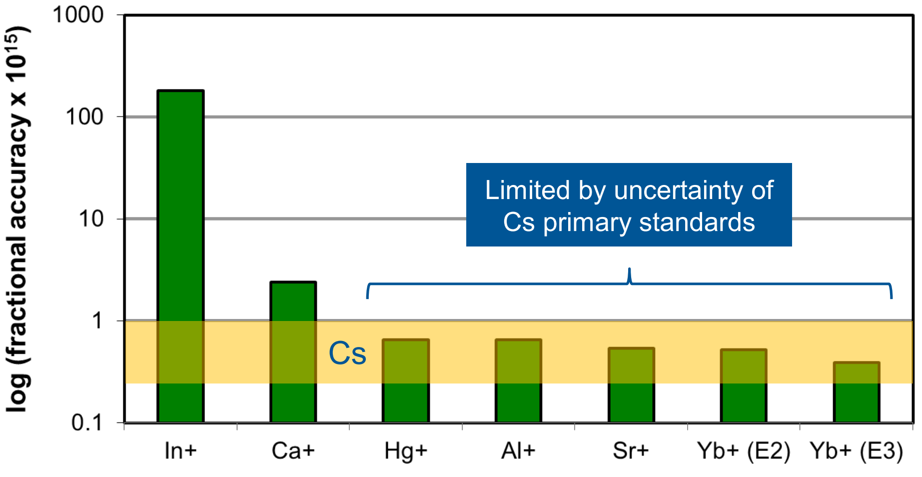

Systematic frequency shifts

Assessing systematic frequency shifts

Measure absolute frequency

Slow and limited in accuracy

Measure shifts relative to a high stability optical local oscillator

By interleaving two independent servos to clock transition

Compare two independent optical frequency standards

Systematic frequency shifts

Zeman shifts
- Due to external magnetic field
- Due to blackbody radiation

Electric quadrupole shift
- Due to electric field gradients

Second-order Doppler shifts
- Due to motion of ion in trap

Stark shifts
- Due to rf trapping field
- Due to applied light fields
- Due to blackbody radiation

Gravitational redshift
- Due to location in Earth's gravitational field

Zeeman shifts in alkali-like ions: odd isotopes

For odd isotope ions with half-integral nuclear spin I,
$m_F = 0 - m_F = 0$ transitions are field independent to first order.

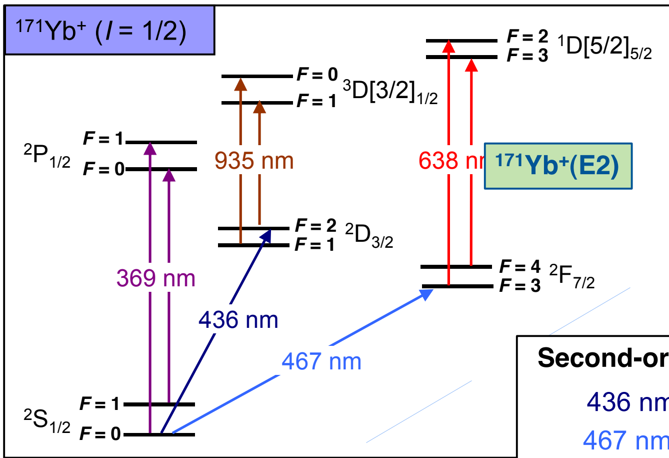

Second-order Zeeman shifts

436 nm: 50 mHz(μT)$^{-2}$

467 nm: 1.7 mHz(μT)$^{-2}$

Zeeman shifts in alkali-like ions: even isotopes

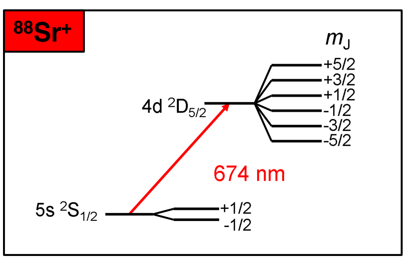

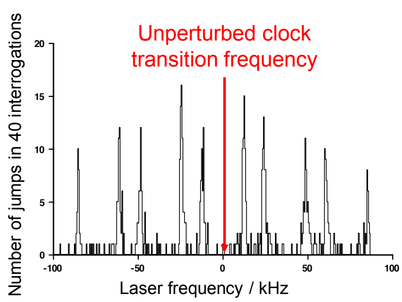

- All components exhibit a linear Zeeman shift
  e.g. 10 kHz μT^{-1} for $^{88}Sr^+$
- 2nd-order Zeeman shift is typically very small
  e.g. 5.6 μHz (μT)$^{-2}$ for innermost components in $^{88}Sr^+$
- Linear Zeeman shift is eliminated by probing two Zeeman components symmetrically placed about line centre

Same procedure used in $^{115}In^+$ and $^{27}Al^+$

Electric quadrupole shift

Due to interaction between electric quadrupole moment of atomic states and any residual electric field gradient at position of ion.

E.g. for $^{88}Sr^{+}$, frequency shift of 4d $^2D_{5/2}$ state with magnetic quantum number m_j is:

$$\Delta\nu = \left(\frac{3}{10h}\right) Q_{dc}\,\Theta(D,5/2)\left(\frac{35}{12} - m_j^2\right)\left(3\cos^2\beta - 1\right)$$

- Q_{dc}: quadrupole field gradient
- $\Theta(D,5/2)$: quadrupole moment of 4d $^2D_{5/2}$ state
- β: angle between quadrupole field axis & magnetic field

Quadrupole trapping potential

$$\phi = (Q_{dc} + Q_{ac}\cos\Omega t)(r^2 - 2z^2)$$

Electric quadrupole moment in $^{88}Sr^{+}$

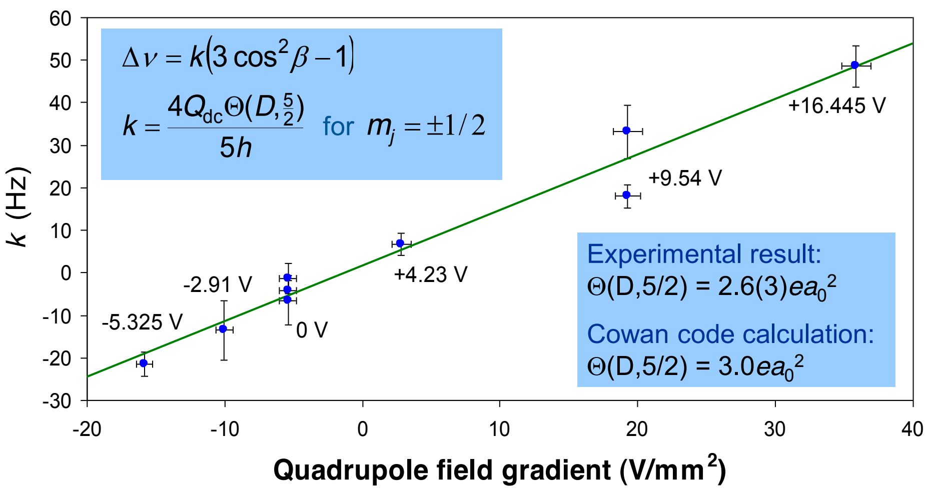

Q_{dc} determined from measurements of the trap secular frequencies

Barwood et al., Phys. Rev. Lett. 93, 133001 (2004)

Quadrupole moments for other systems

NPL | QMI

Ion & state	Quadrupole moment		
	Experiment	Reference	Theory
$^{88}Sr^+\ ^2D_{5/2}$	2.6(3) ea_0^2	G. P. Barwood *et al.*, Phys. Rev. Lett. 93, 133001 (2004)	3.048 ea_0^2 [1]
$^{199}Hg^+\ ^2D_{5/2}$	-0.510(18) ea_0^2	W. H. Oskay *et al.*, Phys. Rev. Lett. 94, 163001 (2005)	-0.56374 ea_0^2 [1]
$^{40}Ca^+\ ^2D_{5/2}$	1.83(1) ea_0^2	C. F. Roos *et al.*, Nature 443, 316 (2006)	1.917 ea_0^2 [1]
$^{171}Yb^+\ ^2D_{3/2}$	2.08(11) ea_0^2	C. Tamm *et al.*, IEEE Trans. Instrum. Meas. 56, 601 (2007)	2.174 ea_0^2 [1]
$^{171}Yb^+\ ^2F_{7/2}$	-0.041(5) ea_0^2	N. Huntemann *et al.*, Phys. Rev. Lett. 108, 090801 (2012)	-0.22 ea_0^2 [2]

Theory: [1] Itano, Phys. Rev. A 73, 022510 (2006)
[2] Blythe et al., J. Phys. B 36, 981 (2003)

No shift in $^{115}In^+$ or $^{27}Al^+$ (J=0 states).

For other systems, shift may be several Hz or more, but can be nulled.

Nulling the quadrupole shift

NPL | QMI

$$\Delta\nu = A\left(\frac{35}{12} - m_j^2\right)\left(3\cos^2\beta - 1\right)$$

Method 1: [Itano, J. Res. Natl. Inst. Stand. Technol. 105, 829 (2000)]

- Carry out frequency measurements for 3 orthogonal magnetic field directions
- Average quadrupole shift is zero

Method 2: [Dubé *et al.*, Phys. Rev. Lett. 95, 033001 (2005)]

- Carry out frequency measurements for Zeeman components corresponding to all different possible $|m_j|$ values
- Average quadrupole shift is zero independent of magnetic field direction

Doppler shifts

First-order Doppler broadening eliminated by laser cooling the ion to the Lamb-Dicke regime

Second-order Doppler shifts arise from two sources:

1. Thermal (secular) motion
   Shift ~10^{-18} if close to the Doppler cooling limit (typically ~1 mK)
2. Micromotion ~10^{-17}
   Careful minimization in 3D vital for reduction below 10^{-17}

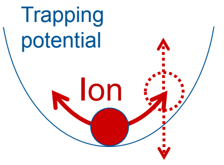

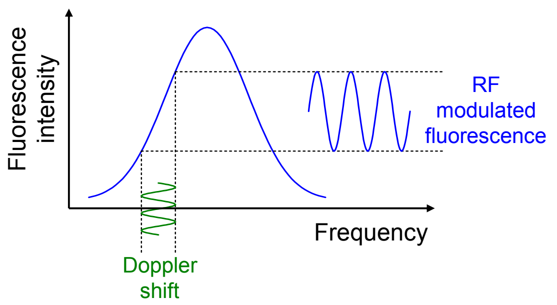

Stark shifts – due to E-field

External electric fields induce a dipole moment in the ion, then interact with that induced dipole as a 2nd order effect (shifts proportional to E^2)

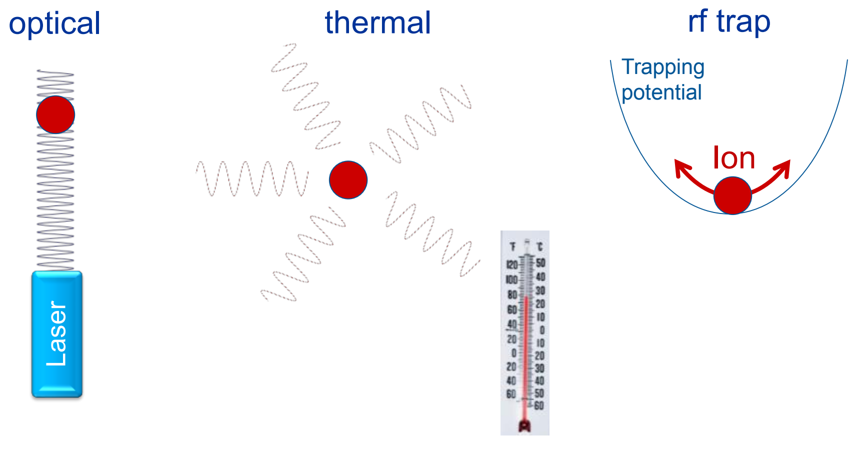

Stark shifts – due to rf trapping E-field

Motion leads to ion experiencing a time-averaged non-zero E field

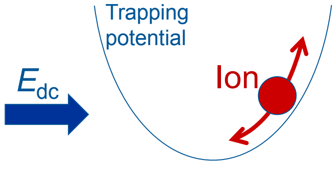

Uncompensated E_{dc} can push ion away from trap centre into higher E_{rf}

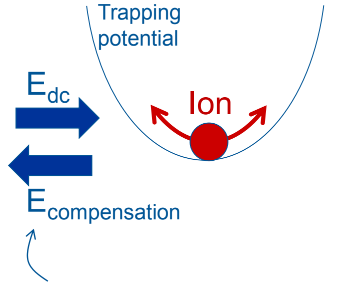

applied with additional electrodes placed near trap

With careful micromotion compensation, shift can be reduced to a few parts in 10^{18}

Stark shifts from applied laser fields

- High extinction of cooling (and repumper) beams is vital
- Negligible shift due to probe laser at typical intensities used
- Current exception is 467 nm electric octupole transition in $^{171}Yb^{+}$

Probe beam:
~ 6 mW, ~ 25 μm radius

➡ ac Stark shift ~ 200 Hz

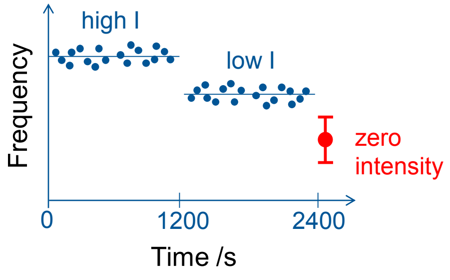

- Fractional uncertainty of 4.2×10^{-17} reached using this method
- Could be further reduced with narrower probe laser linewidths

Blackbody Stark shifts

Typically 100 – 500 mHz at room temperature

Two contributions to uncertainty:

- Uncertainty in Stark shift coefficients
  - Main contribution is from static differential polarizability of reference transition (resonant contributions are small)
- Uncertainty in temperature and isotropy of radiation field experienced by ion
  - Significant temperature rises of electrode structure have been observed for some trap designs
  - Effect of non-isotropic temperature distribution can be suppressed by designing electrodes to have low emissivity

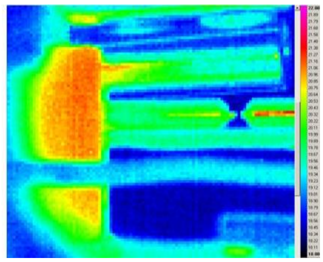

Thermal image of trapping region (18-22ºC)

Gravitational redshift

Frequency shift $\frac{\Delta f}{f} = \frac{g\Delta h}{c^2}$

g = local acceleration due to gravity
Δh = height above reference level
c = speed of light

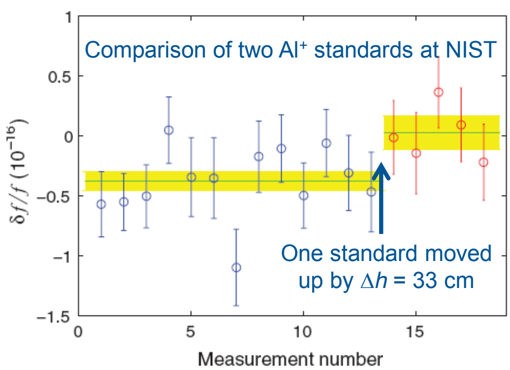

Measured

$$\frac{\Delta f}{f} = (4.1 \pm 1.6) \times 10^{-17}$$

corresponding to

$$\Delta h = 37 \pm 15 \text{ cm}$$

Chou et al., Science 329, 1630 (2010)

Effect in the laboratory is very small but must be taken into account when comparing frequency standards in different laboratories

Current status of optical clocks and prerequisites for a redefinition of the SI second

Improvements in optical clocks

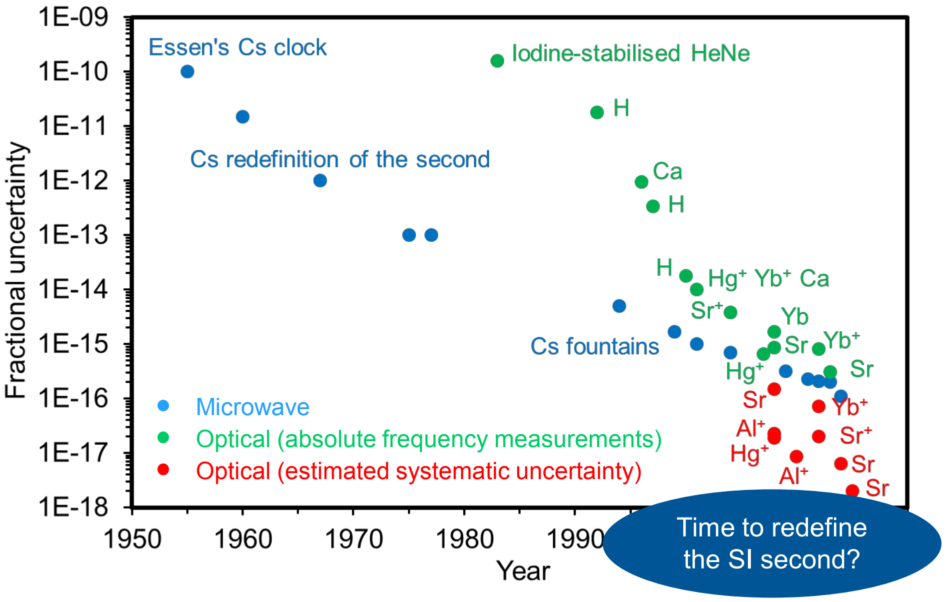

Secondary representations of the second

- Optical frequency standards can be used to realise the SI second (although uncertainty cannot be better than Cs primary standard)
- List of secondary representations of the second now includes seven optical frequency standards

Atom or ion	Transition	Wavelength	Recommended fractional uncertainty
^{87}Sr	$^1S_0 - {}^3P_0$	698 nm	1.0×10^{-15}
$^{171}Yb^+$	$^2S_{1/2} - {}^2F_{7/2}$	467 nm	1.3×10^{-15}
$^{27}Al^+$	$^1S_0 - {}^3P_0$	267 nm	1.9×10^{-15}
$^{199}Hg^+$	$^2S_{1/2} - {}^2D_{5/2}$	282 nm	1.9×10^{-15}
^{171}Yb	$^1S_0 - {}^3P_0$	578 nm	2.7×10^{-15}
$^{171}Yb^+$	$^2S_{1/2} - {}^2D_{3/2}$	436 nm	3.0×10^{-15}
$^{88}Sr^+$	$^2S_{1/2} - {}^2D_{5/2}$	674 nm	4.0×10^{-15}

Integration of optical clocks into UTC

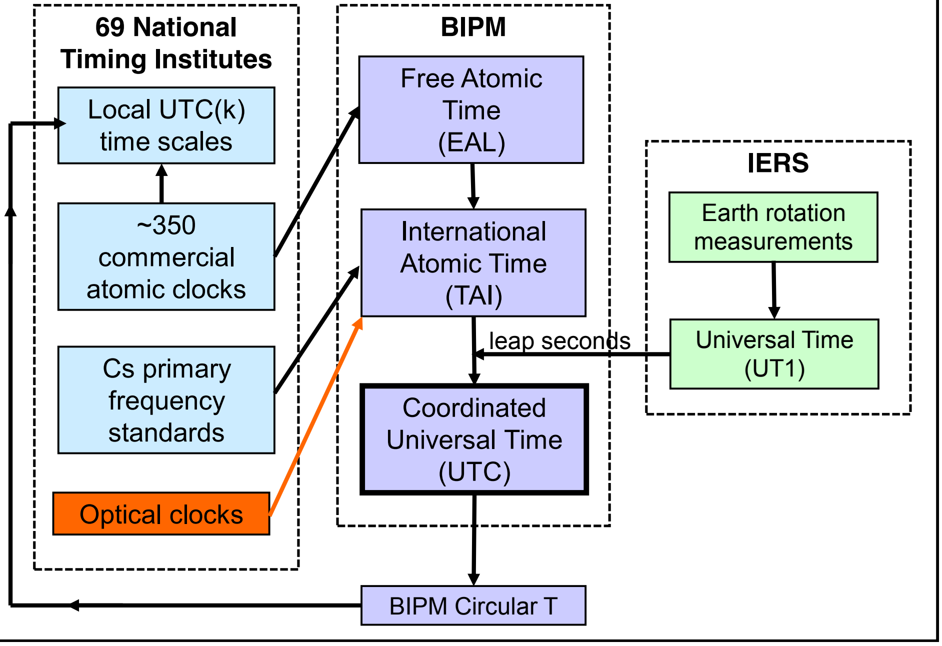

Local comparisons: stability

Comparison between two ^{171}Yb lattice clocks at NIST:

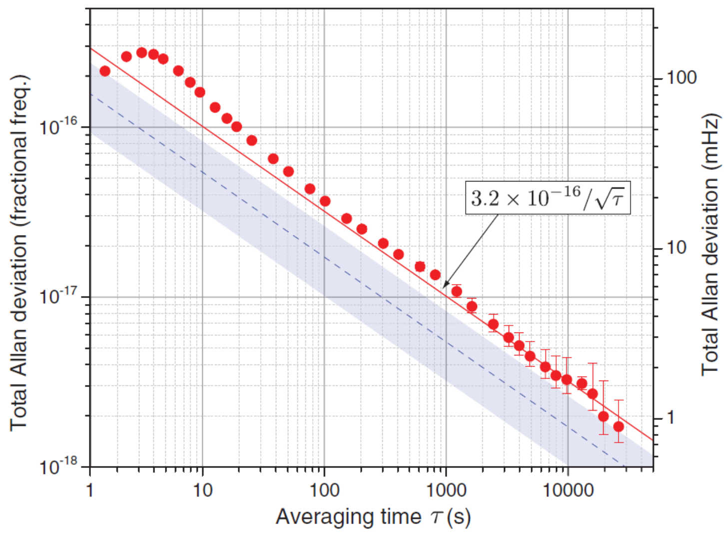

Hinkley *et al.*, Science 341, 1215 (2013)

Local comparisons: reproducibility

Comparison of two $^{27}Al^{+}$ standards at NIST:

$^{27}Al^{+}$ / $^{9}Be^{+}$ $u_B \sim 2.3 \times 10^{-17}$
$^{27}Al^{+}$ / $^{25}Mg^{+}$ $u_B \sim 8.6 \times 10^{-18}$

Fractional frequency difference
$-1.8\ (\pm 0.7) \times 10^{-17}$

Chou *et al.*, PRL 104, 070802 (2010)

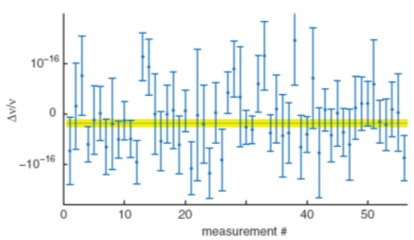

Comparison of two cryogenic ^{87}Sr lattice clocks at RIKEN:

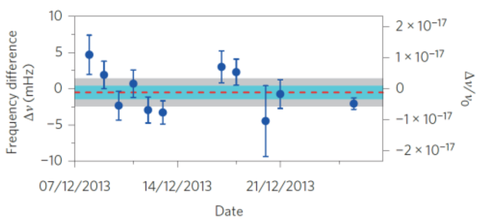

Fractional frequency difference
$(-1.1 \pm 2.0(\text{stat}) \pm 4.4(\text{syst})) \times 10^{-18}$

Ushijima *et al.*, Nature Photonics 9, 183 (2015)

International comparisons: $^{171}Yb^{+}$ E3

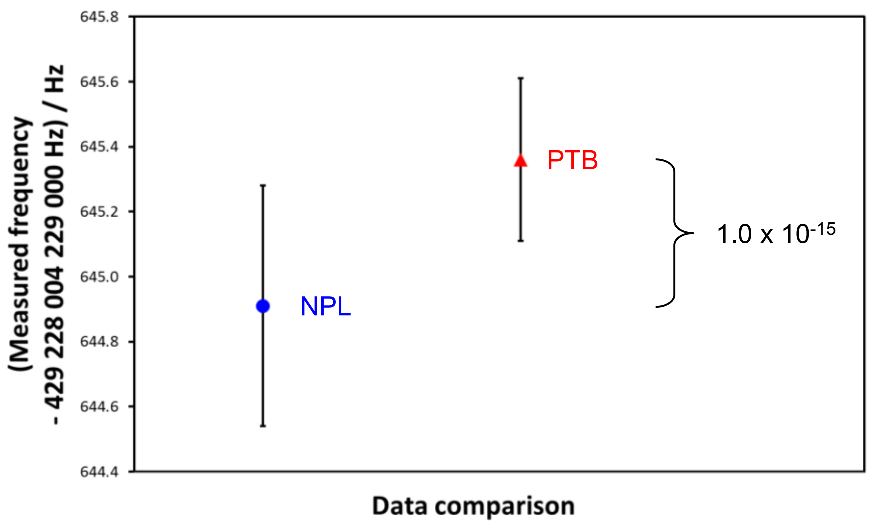

Independent absolute frequency measurements made relative to local Cs fountain primary frequency standards

International comparisons: ^{87}Sr

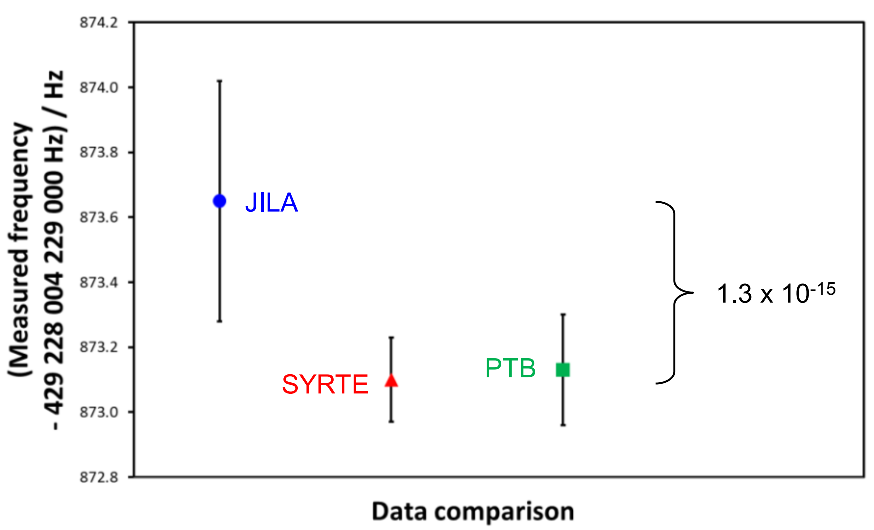

Independent absolute frequency measurements made relative to local Cs fountain primary frequency standards

Prerequisites for a redefinition

- Ultimate limits to the stability and accuracy of optical clocks fully investigated
- Improved methods for comparing optical clocks developed in different laboratories
- A coordinated programme of clock comparisons, to
  - Build confidence in the optical clocks
  - Anchor their frequencies to the current definition of the second
  - Establish the leading contenders for a redefinition
- Evaluation of relativistic effects at an improved level of accuracy
  - Includes the gravitational redshift of the clock frequency
- A framework and procedures for the optical clocks to be integrated into international timescales

Outline (Part 2)

Clock comparison techniques

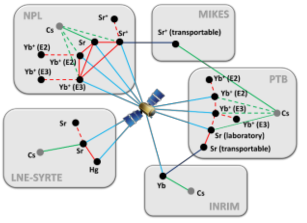

- Local frequency comparisons
  - Optical frequency ratio measurements
  - Absolute frequency measurements
- Remote optical frequency comparisons
  - Transportable optical clocks
  - Satellite-based techniques
  - Comparisons over optical fibre links
- Handling over-determined sets of clock comparison data

Optical atomic clocks, relativity and geodesy

- Gravity potential for optical clock comparisons
- Clock-based geodesy

Fundamental physics with optical clocks

Prerequisites for a redefinition

- Ultimate limits to the stability and accuracy of optical clocks fully investigated
- Improved methods for comparing optical clocks developed in different laboratories
- A coordinated programme of clock comparisons, to
  - Build confidence in the optical clocks
  - Anchor their frequencies to the current definition of the second
  - Establish the leading contenders for a redefinition
- Evaluation of relativistic effects at an improved level of accuracy
  - Includes the gravitational redshift of the clock frequency
- A framework and procedures for the optical clocks to be integrated into international timescales

ITOC clock comparison programme

ITOC

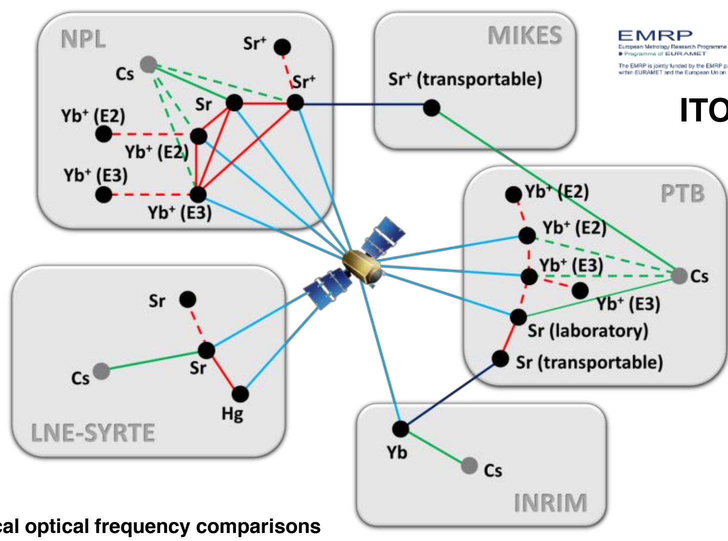

- Local optical frequency comparisons
- Frequency comparisons using transportable optical clocks
- Optical frequency comparisons using broad bandwidth TWSTFT
- Absolute frequency measurements

Local frequency comparisons

Self-referenced optical frequency comb

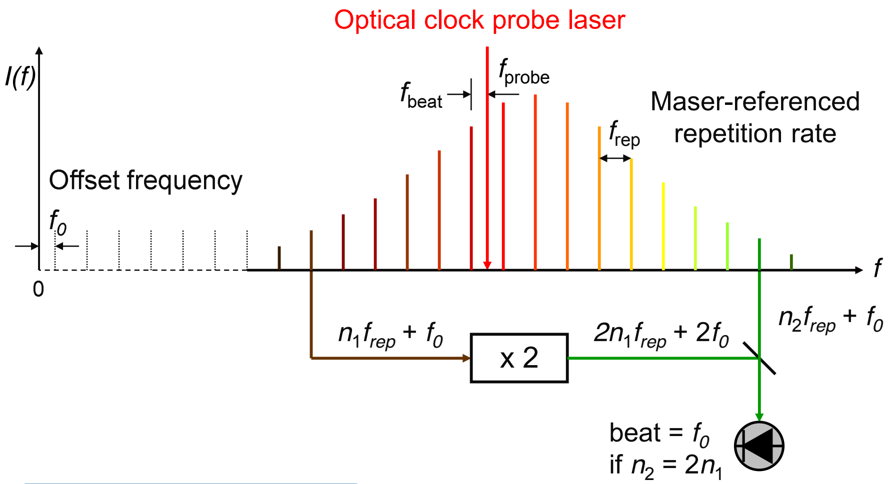

$f_{probe} = m\, f_{rep} \pm f_0 \pm f_{beat}$

Linking clocks within NPL

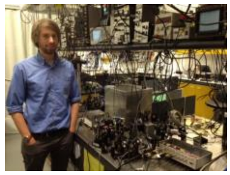

Strontium optical lattice clock

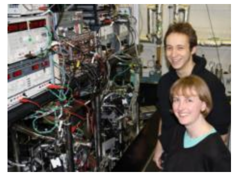

Ytterbium ion optical clock

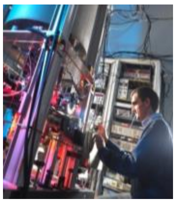

Caesium fountain

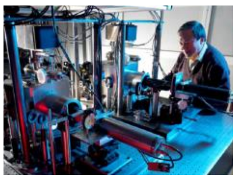

Strontium ion optical clock

Femtosecond combs used for

- Absolute frequency measurements
- Optical frequency ratio measurements

Checking the comb accuracy

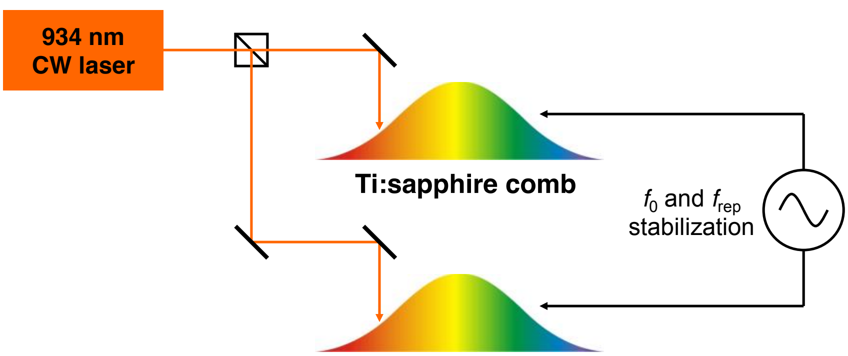

Measure the same optical frequency using two independent combs referenced to a common microwave source

→ fluctuations in cw laser frequency cancel

→ fluctuations in microwave reference frequency cancel

Checking the comb accuracy

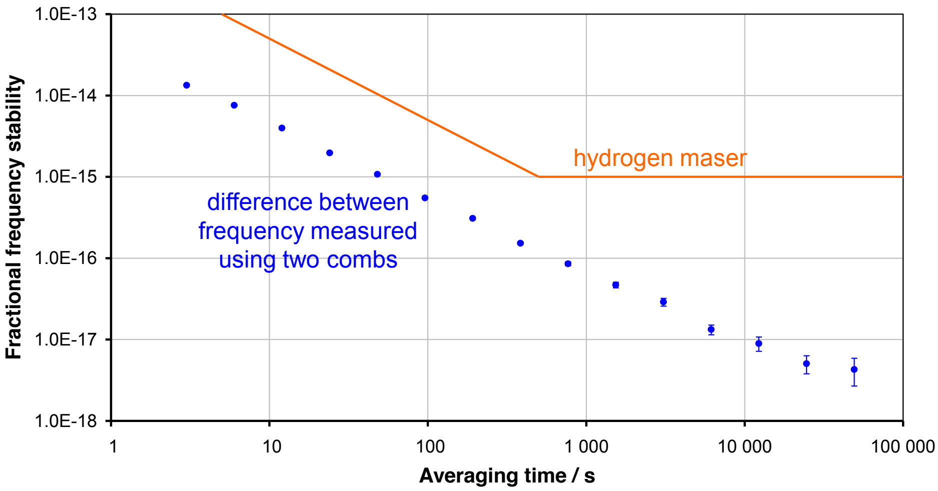

Noise of hydrogen maser is suppressed in the comparison

Checking the comb accuracy

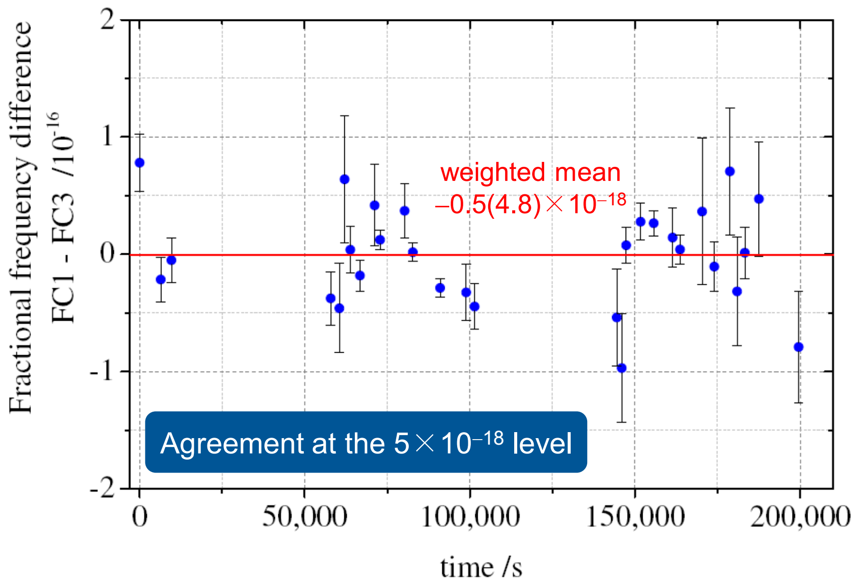

L. A. M. Johnson, P. Gill and H. S. Margolis, Metrologia 52, 62 (2015)

Measuring optical frequency ratios

Frequency ratio

$$\frac{f_2}{f_1} = \frac{m_2 f_{rep} + f_0 + f_{b2}}{m_1 f_{rep} + f_0 + f_{b1}}$$

$$= \frac{m_2}{m_1}\left(\frac{1 + \Delta_2}{1 + \Delta_1}\right)$$

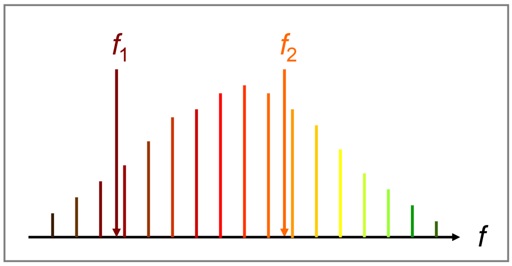

i.e. f_{rep} cancels to first order, so optical frequency ratios can be measured more accurately than absolute frequencies.

$$\Delta_i = \left(\frac{f_0 + f_{bi}}{m_i f_{rep}}\right) \sim 10^{-6} - 10^{-7}$$

so to determine f_2 / f_1 with a fractional uncertainty of 10^{-18}, Δ_i only has to be measured to a fractional accuracy of $10^{-11} - 10^{-12}$.

Checking the comb accuracy

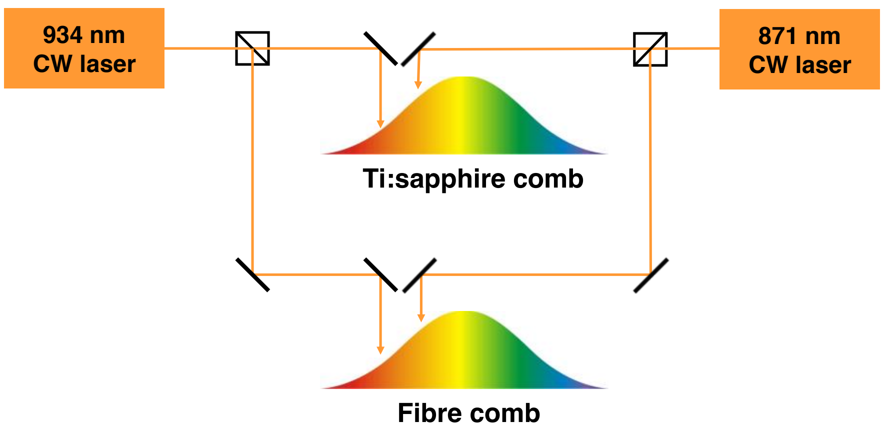

Same optical frequency ratio measured using two independent combs

Checking the comb accuracy

NPL National Physical Laboratory | QMI Quantum Metrology Institute

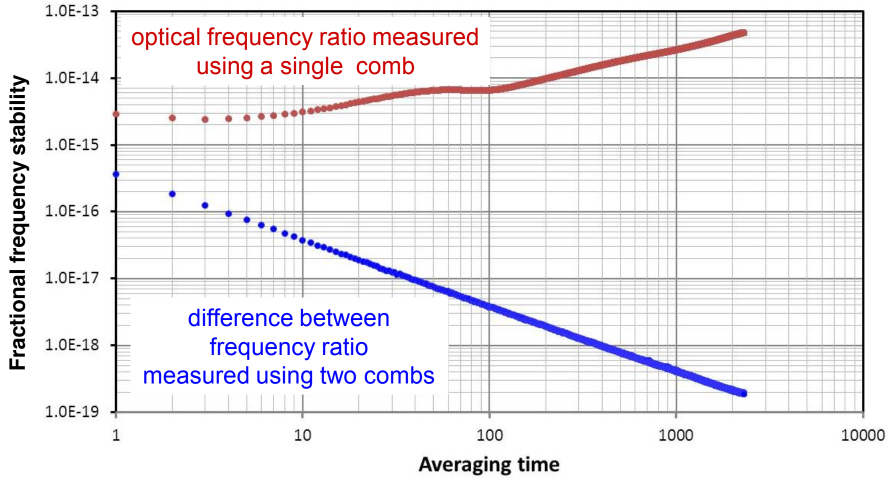

Instabilities of the cw lasers are common mode and are suppressed

Checking the comb accuracy

NPL National Physical Laboratory | QMI Quantum Metrology Institute

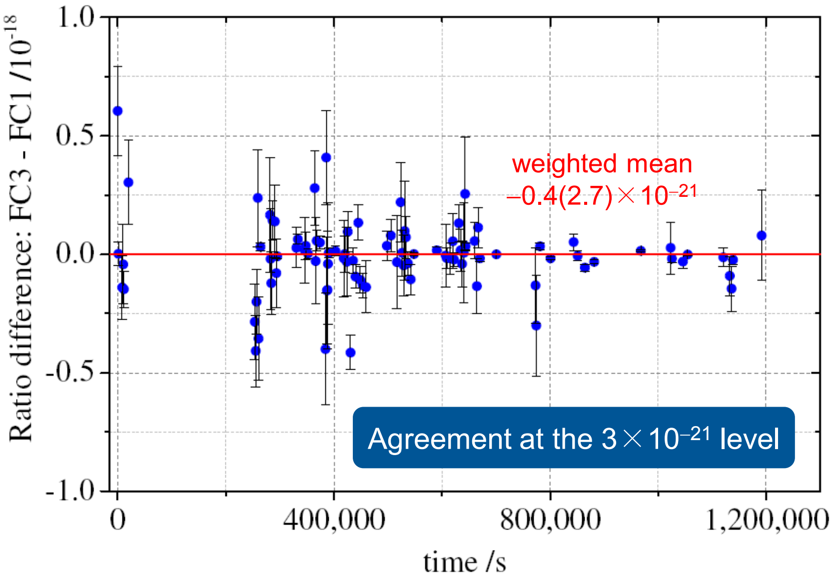

L. A. M. Johnson, P. Gill and H. S. Margolis, Metrologia 52, 62 (2015)

Measurements in $^{171}Yb^{+}$

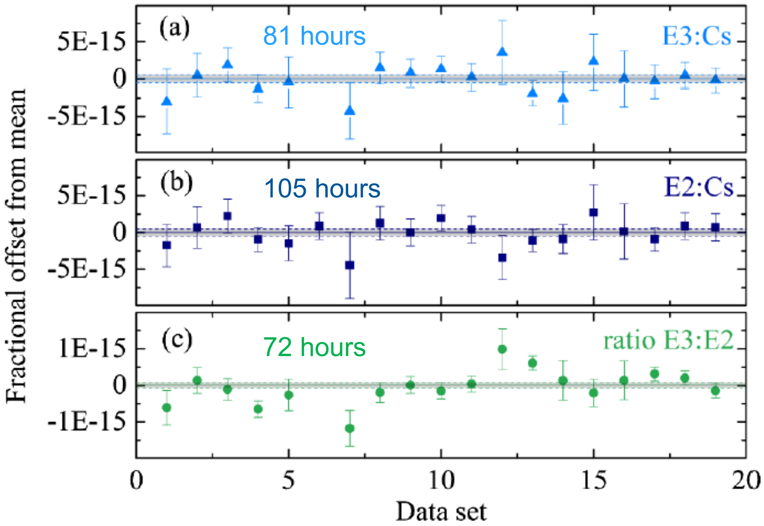

Uncertainty 5.8×10^{-16}

Uncertainty 6.1×10^{-16}

Uncertainty 3.3×10^{-16} (Statistical 7×10^{-17})

Godun *et al.*, Phys. Rev. Lett. 113, 210801 (2014)

Other optical frequency ratio measurements

ν_{Al+} / ν_{Hg+}

Fractional uncertainty 5.2×10^{-17}

Rosenband *et al.*, Science 319, 1808 (2008)

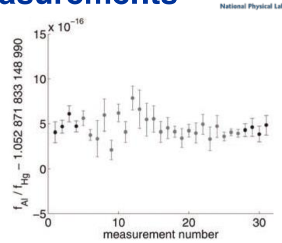

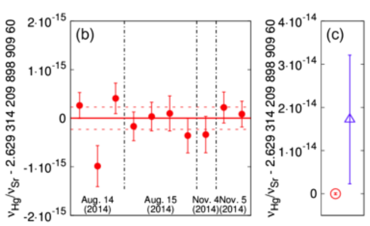

ν_{Hg} / ν_{Sr}

Fractional uncertainty 8.4×10^{-17}

Yamanaka *et al.*, PRL 114, 230801 (2015)

ν_{Yb} / ν_{Sr}

Fractional uncertainty 4.6×10^{-17}

Nemitz *et al.*, arXiv:1601.04582 (2016)

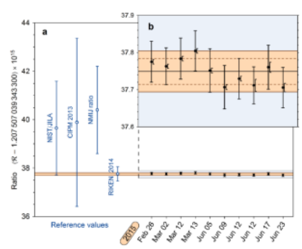

Absolute frequency measurements: ITOC

NPL
$^{88}Sr^{+}$ – 1 measurement
$^{171}Yb^{+}$ E3 – 1 measurement *
$^{171}Yb^{+}$ E2 – 1 measurement *
^{87}Sr – 1 measurement

MIKES
$^{88}Sr^{+}$ – 1 measurement

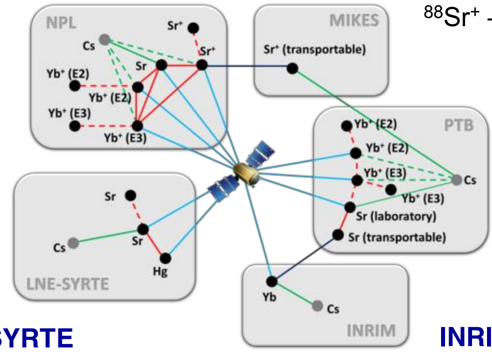

PTB
^{87}Sr – 1 measurement
$^{171}Yb^{+}$ E3 – 1 measurement *
$^{171}Yb^{+}$ E2 – 1 measurement *

LNE-SYRTE
^{87}Sr – 1 measurement

INRIM
^{171}Yb – 1 measurement

* From EMRP project “High accuracy optical clocks with trapped ions”

Local optical ratio measurements: ITOC

NPL
$^{171}Yb^{+}$ E3 / $^{171}Yb^{+}$ E2 – 1 measurement *
$^{171}Yb^{+}$ E3 / ^{87}Sr – 1 measurement
$^{171}Yb^{+}$ E3 / $^{88}Sr^{+}$ / ^{87}Sr – 1 measurement
$^{171}Yb^{+}$ E3 / $^{171}Yb^{+}$ E2 – 1 measurement

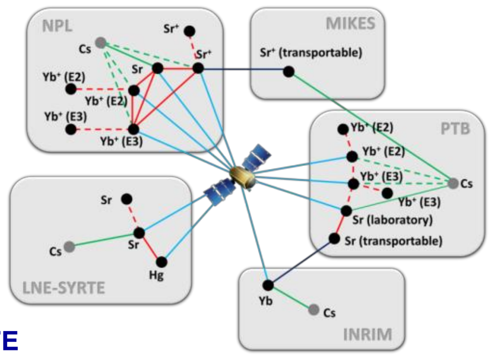

PTB
$^{171}Yb^{+}$ E3 / ^{87}Sr
– 1 measurement *

LNE-SYRTE
^{87}Sr / Hg – 2 measurements

* From EMRP project “High accuracy optical clocks with trapped ions”

Remote optical frequency comparisons

Transportable optical clocks

Two transportable optical clocks are being developed within the ITOC project, at PTB and MIKES

Transportable optical clocks **Stationary optical clocks**

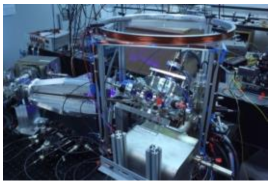

Strontium lattice, PTB

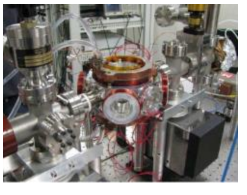

Ytterbium lattice, INRIM

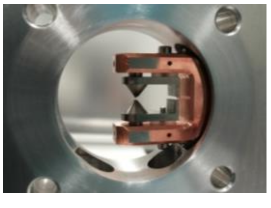

Strontium ion, MIKES

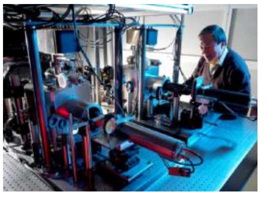

Strontium ion, NPL

PTB transportable strontium lattice clock

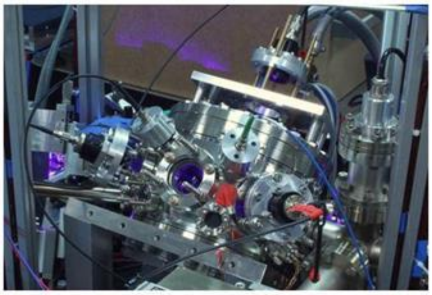

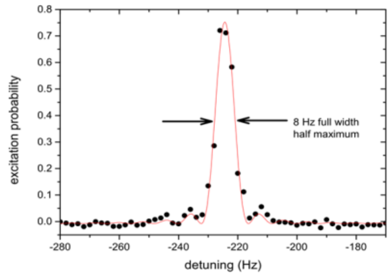

- ^{87}Sr clock transition resolved with sub-10 Hz linewidth and high contrast
- Observed stability in preliminary comparisons against laboratory lattice clock well within design expectations
- Clock has now been transported for the first time!

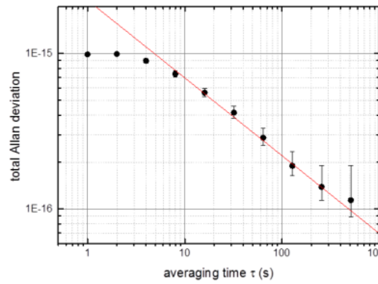

SOC2: towards space optical clocks

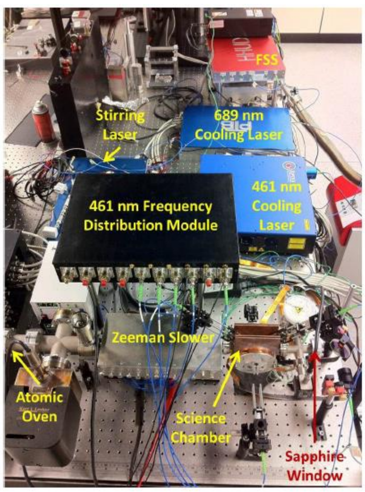

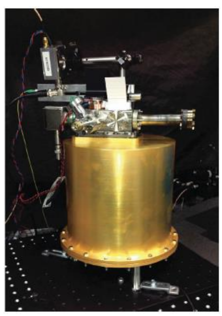

- ^{87}Sr optical lattice clock
- Modular design consisting of compact subunits

Target performance:

Fractional instability $\sigma < 1 \times 10^{-15}\,\tau^{-1/2}$

Fractional inaccuracy $< 5 \times 10^{-17}$

EU project coordinated by Prof. Stephan Schiller, University of Düsseldorf

Bongs *et al*, C. R. Physique 16, 553 (2015)

Two-way satellite time and frequency transfer

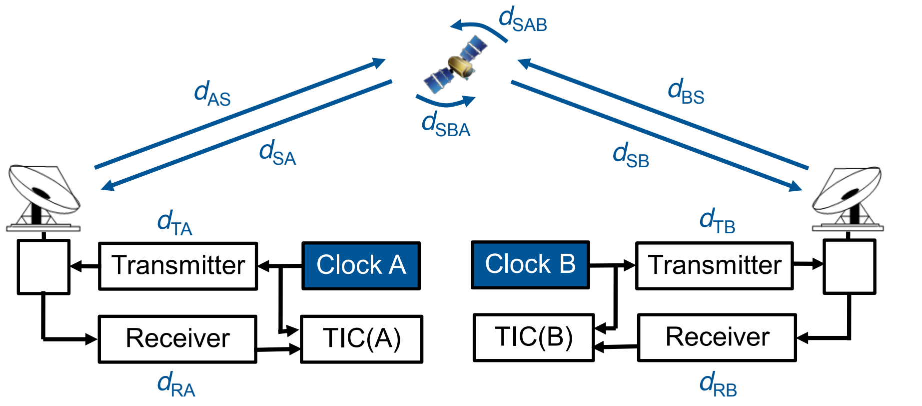

$$A - B = [TIC(A) - TIC(B)]/2 + (d_{TA} - d_{RA})/2 - (d_{TB} - d_{RB})/2$$
$$+ (d_{AS} - d_{SA})/2 - (d_{BS} - d_{SB})/2 + (d_{SAB} - d_{SBA})/2 - 2\omega A/c^2$$

Propagation delays tend to cancel, but not exactly if different frequencies are used for up and down links

Satellite delays cancel if same transponder is used for both directions

Optical clock comparisons via satellite

NICT – PTB

Carrier-phase-based two-way satellite time and frequency transfer (TWCP)

Remote comparison of ^{87}Sr lattice clocks separated by a baseline of 9000 km

Fractional difference $(1.1 \pm 1.6) \times 10^{-15}$

Hachisu *et al*, Opt. Lett. 39, 4072 (2014)

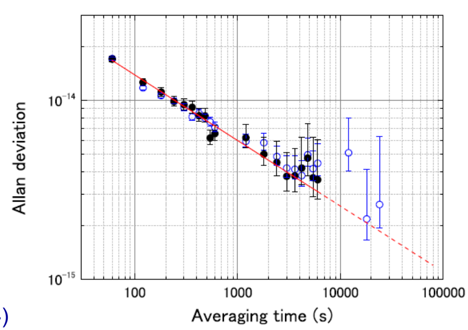

Optical clock comparisons via satellite

NPL | QMI

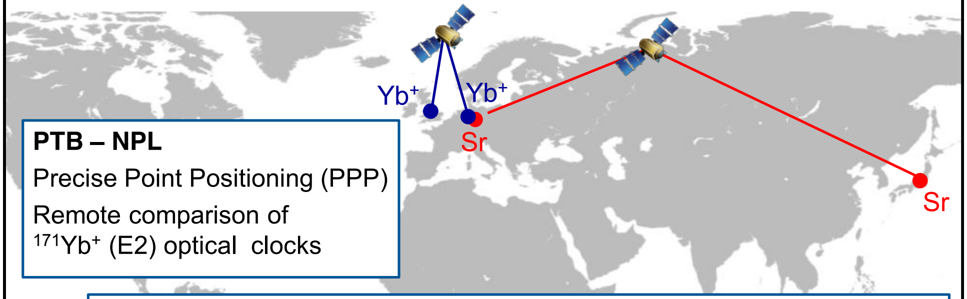

PTB – NPL

Precise Point Positioning (PPP)

Remote comparison of $^{171}Yb^+$ (E2) optical clocks

NICT – PTB

Carrier-phase-based two-way satellite time and frequency transfer (TWCP)

Remote comparison of ^{87}Sr lattice clocks separated by a baseline of 9000 km

Fractional difference $(1.1 \pm 1.6) \times 10^{-15}$

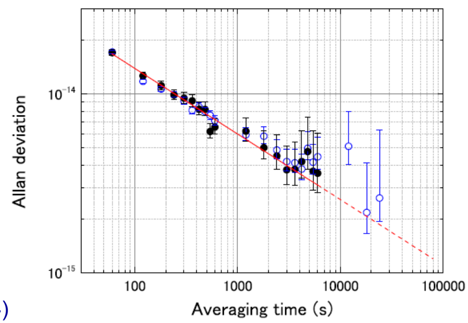

Hachisu *et al*, Opt. Lett. 39, 4072 (2014)

$^{171}Yb^+$ optical clock comparison via GPS PPP

NPL | QMI | PTB | VTT MIKES METROLOGY

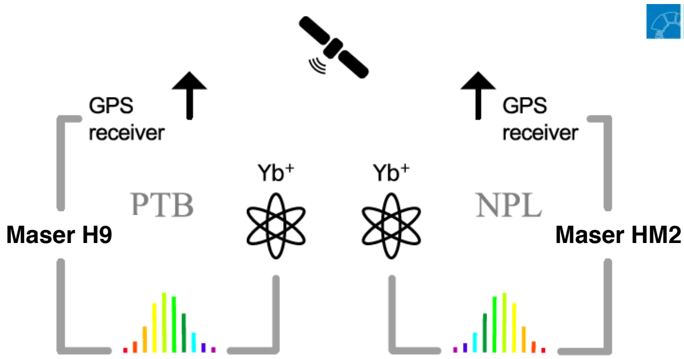

- Hydrogen maser as flywheel oscillator in each laboratory
- Maser connected to GPS receiver as an external reference and simultaneously compared to $^{171}Yb^+$ standard via a frequency comb
- Maser and IGS time contributions cancel out if no gaps in data and no inherent dead-time

$^{171}Yb^+$ optical clock comparison via GPS PPP

However

- Both optical clock vs maser data sets contain gaps
- NPL data-taking method led to an inherent dead-time of 10%

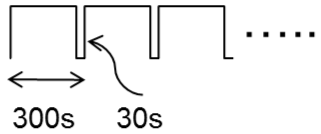

Two possible solutions:

1) Only consider time intervals where data is available from both clocks
   - Fragments the GPS link data, destroying the phase coherence of the measurement
2) Extrapolate the optical clock data to intervals where GPS link data is available but data from one or both clocks is missing
   - Introduces maser noise to the frequency comparison

$^{171}Yb^+$ optical clock comparison via GPS PPP

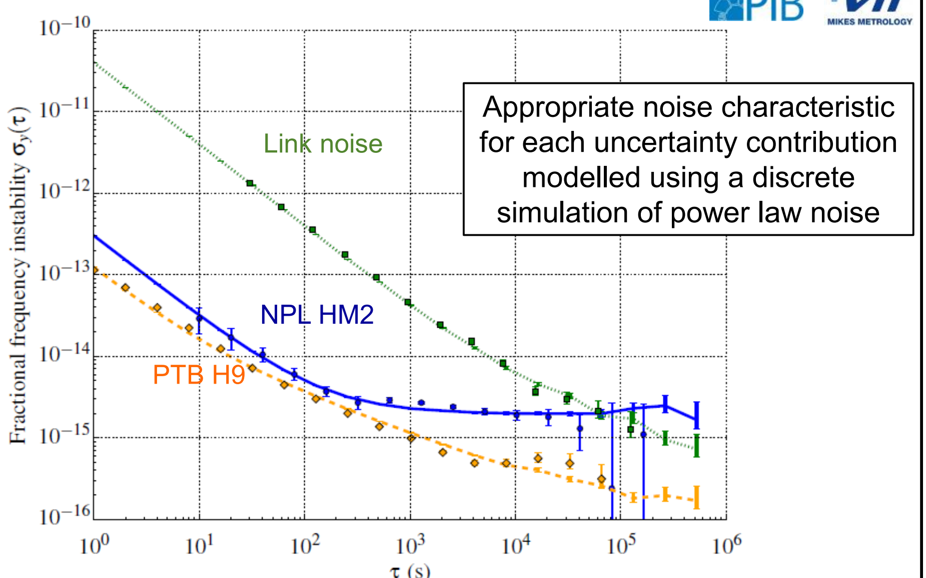

Modelling performed by Julia Leute, PTB

$^{171}Yb^{+}$ optical clock comparison via GPS PPP

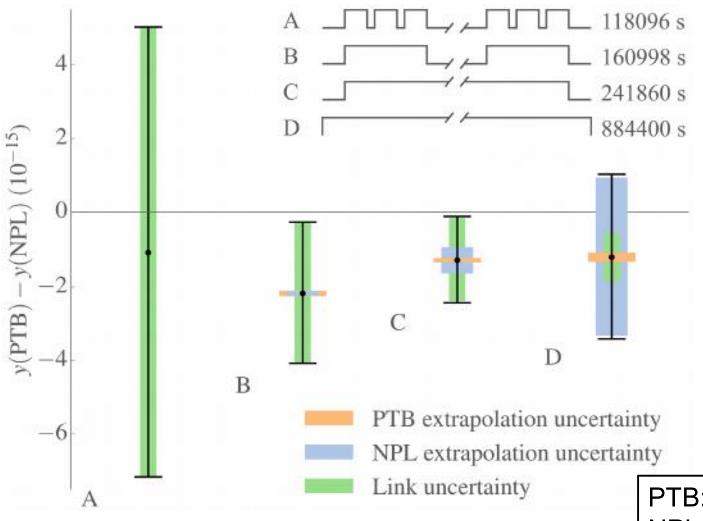

PTB: 130 hours
NPL: 46 hours
Overlap: 33 hours

$^{171}Yb^{+}$ optical clock comparison via GPS PPP

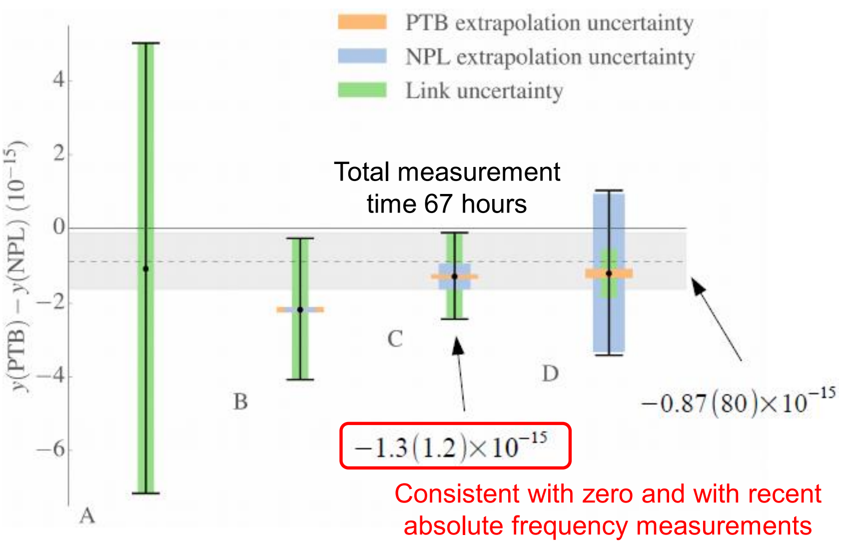

Consistent with zero and with recent absolute frequency measurements

Leute et al., accepted for publication in IEEE Trans. UFFC (2016)

Optical clock comparisons via broadband TWSTFT

- Investigation of improved TWSTFT technique based on an increased chip rate

  1 Mchip / s → 20 Mchip / s

- Goal is a gain in stability of one order of magnitude compared to state-of-the-art satellite-based methods

  10^{-15} @ 1 day → 10^{-16} @ 1 day

- Link test (7 days, October 2014) followed by optical clock comparisons (21 days, June 2015)
- Comparisons of clocks in all four laboratories with TWSTF capability (INRIM, LNE-SYRTE, NPL, PTB)

  Cs fountains as well as optical clocks

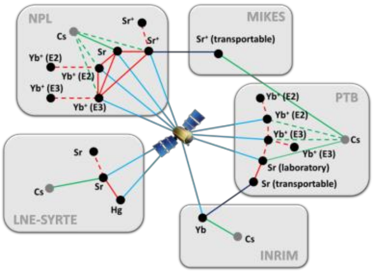

Link test results

One-week link test in October 2014 using SES ASTRA 3B satellite

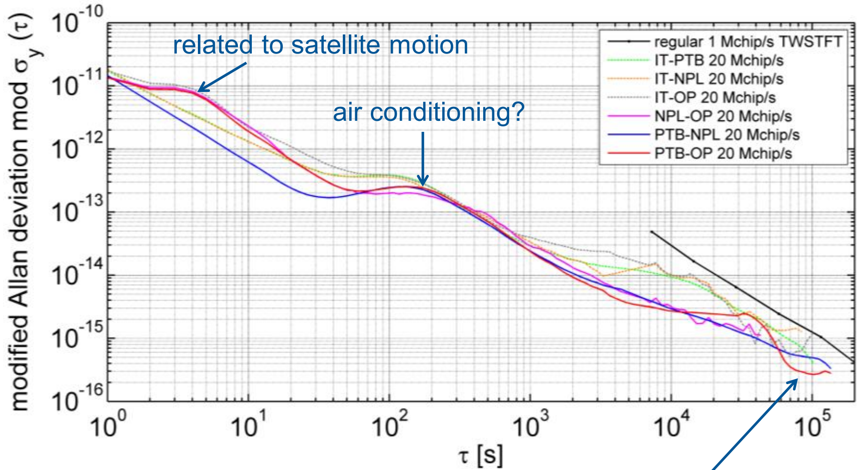

Instabilities of a few parts in 10^{16} at one day (MDEV)
Limited by stability of hydrogen masers

Clock comparison campaign

NPL	Yb^+ E3, Sr^+, Sr
PTB	Yb^+ E3, Sr
OP	Sr, Hg
INRIM	Yb

4th – ~~25th~~ 29th June 2015

Duty cycles for optical clocks were typically in the range 60–80%:

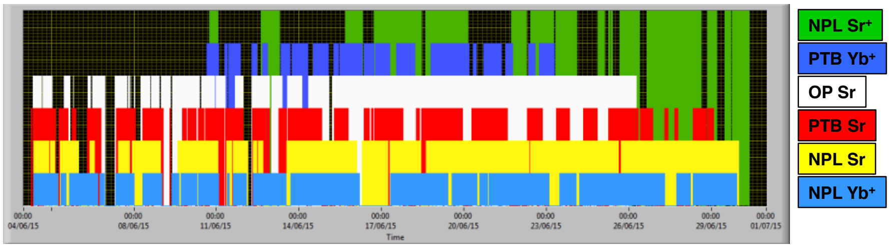

… data analysis is still being finalised!

ACES Microwave Link

Part of the payload to be installed on the International Space Station

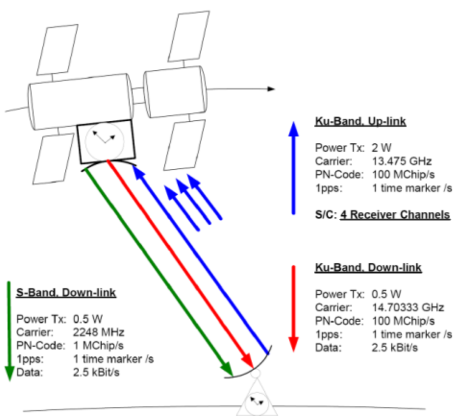

- Bi-directional K_u-band link with high modulation rate of 100 MChips/s
- Additional S-band downlink allows ionospheriic delay to be determined and cancelled

Specified performance ADEV $\leq 1.6 \times 10^{-16}$ @ 1 day, but intercontinental frequency comparison accuracies at the 10^{-17} level achievable with one week of averaging if no cycle slips

Frequency dissemination via optical fibres

NPL | QMI

Wavelength / nm	Attenuation / dB km^{-1}
630	12
780	4
1060	1.5
1310	0.33
1550	0.2

Use the 1.5 µm transmission band of standard telecommunications fibre

Attenuation @ 1550 nm: 20 – 25 dB per 100 km

3 techniques for high stability frequency transfer investigated:

1. **Microwave** — Transfer of an amplitude-modulated CW laser
2. **Optical** — Transfer of a stabilized CW laser
3. **Microwave + Optical** — Transfer of an optical frequency comb

Choice of optical carrier frequency

NPL | QMI

Challenge: Link attenuation is lowest at 1550 nm but optical clocks operate in the visible or UV

Solution: Use a frequency comb at each end of the link to relate the frequency of a 1550 nm transfer laser to that of the local optical clock

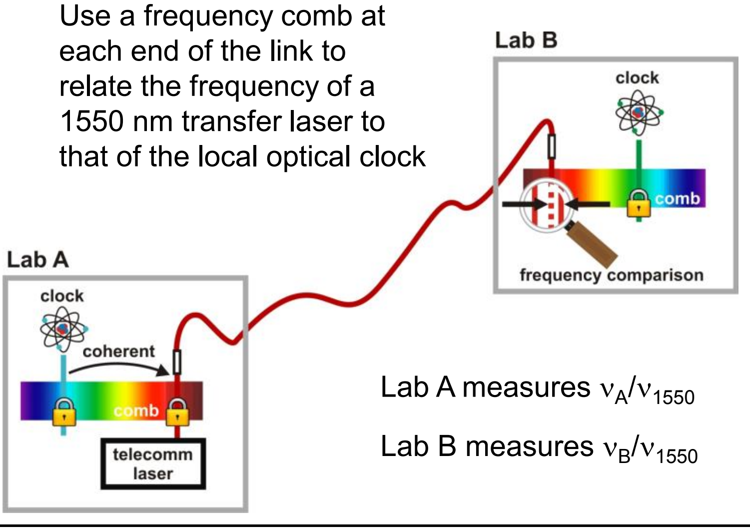

Lab A measures ν_A/ν_{1550}

Lab B measures ν_B/ν_{1550}

Environmental effects

Challenge: Fibres are affected by noise from the environment

➡ degrades the phase and amplitude stability of the transmitted signal

Sources of noise
- Vibrations
- Temperature changes

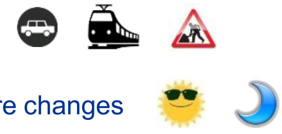

Solution: (1) For good thermal, acoustic and seismic isolation use underground fibre

(2) Use active noise cancellation techniques

Fibre noise cancellation

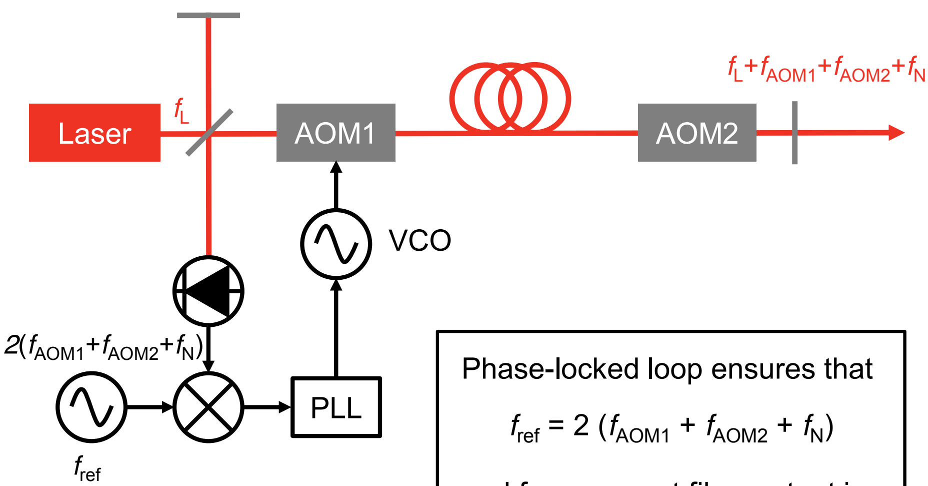

Phase-locked loop ensures that

$$f_{ref} = 2\,(f_{AOM1} + f_{AOM2} + f_N)$$

and frequency at fibre output is

$$f_L + (f_{ref} / 2)$$

Ma *et al*., Opt. Lett. 19, 1777 (1994)

Limitations

$S_\phi^{\text{reference path}}$ Keep it short and well isolated

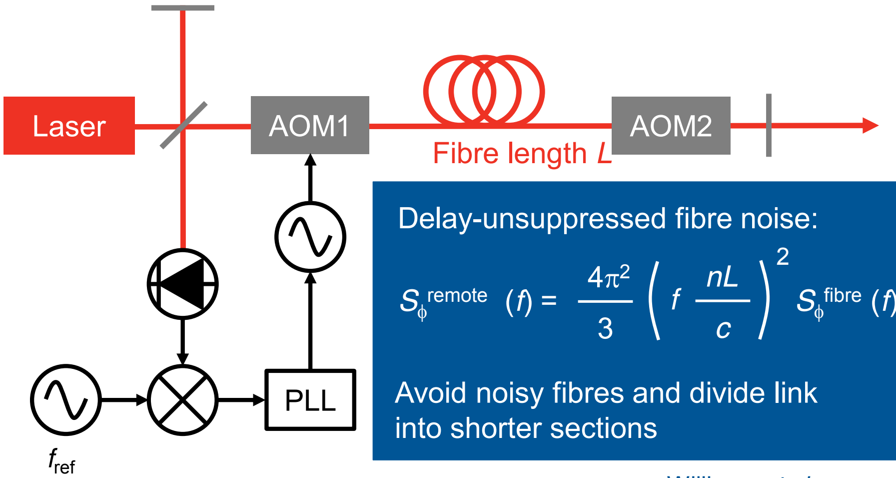

Delay-unsuppressed fibre noise:

$$S_\phi^{\text{remote}}(f) = \frac{4\pi^2}{3}\left(f\,\frac{nL}{c}\right)^2 S_\phi^{\text{fibre}}(f)$$

Avoid noisy fibres and divide link into shorter sections

S_ϕ^{laser} Stabilise so coherence length > $2L$

Williams *et al.*, JOSA B 25, 1284 (2008)

State-of-the-art performance

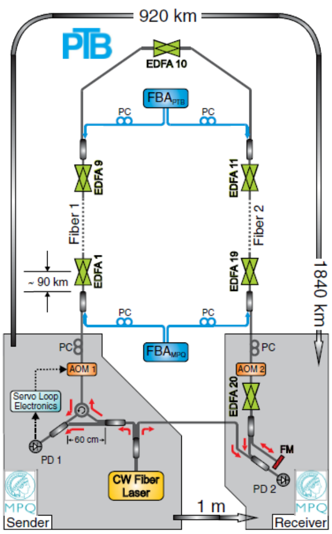

1840 km link MPQ – PTB - MPQ

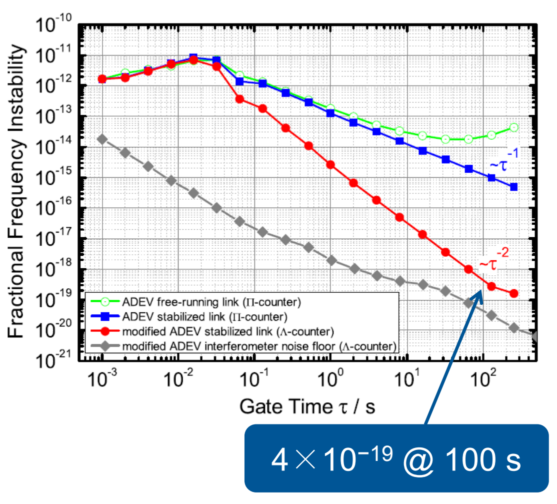

Droste *et al.*, PRL 111, 110801 (2013)

Optical clock comparisons via fibre links

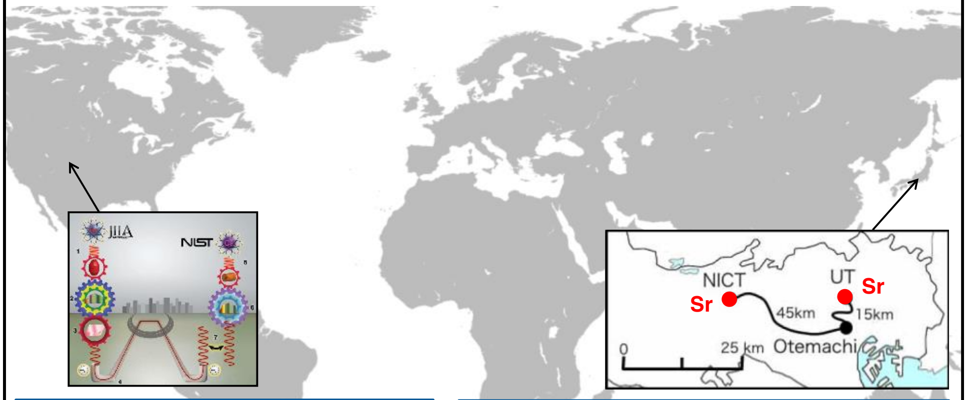

JILA – NIST

4 km fibre link

Uncertainty of ^{87}Sr lattice clock evaluated at the 1×10^{-16} level by remote comparison with a Ca clock

Ludlow *et al*, Science 319, 1805 (2008)

NICT – University of Tokyo

60 km fibre link

Remote comparison of ^{87}Sr lattice clocks; fractional difference $(1.0 \pm 7.3) \times 10^{-16}$

Fujieda *et al*, Opt. Express 19, 16498 (2011)

Yamaguchi *et al*, Appl. Phys. Express 4, 082203 (2011)

Optical clock comparisons via fibre

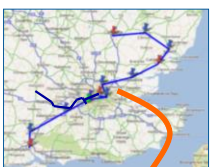

JANET-Aurora

Dark fibre research network

Harwell-NPL-Telehouse North dark fibre links

PTB – Strasbourg link

London – Paris link (GÉANT legacy fibre)

PTB - MPQ

900 km dark fibre

REFIMEVE+ (collaboration with RENATER)

NEAT-FT

LIFT

Italian Fibre Link for Frequency and Time

PTB–SYRTE Sr lattice clock comparison

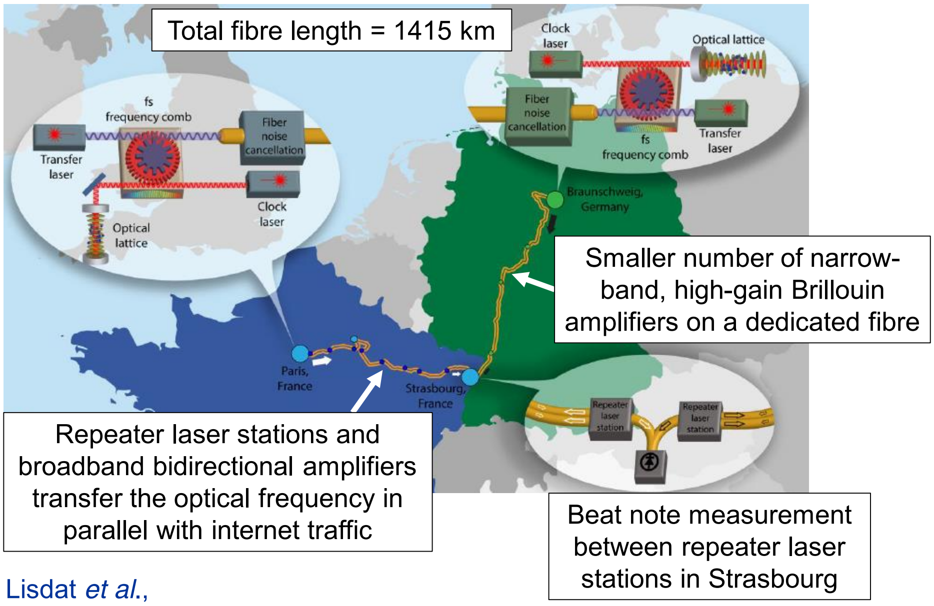

Lisdat *et al.*,
arXiv: 1511.07735 (2015)

PTB–SYRTE Sr lattice clock comparison

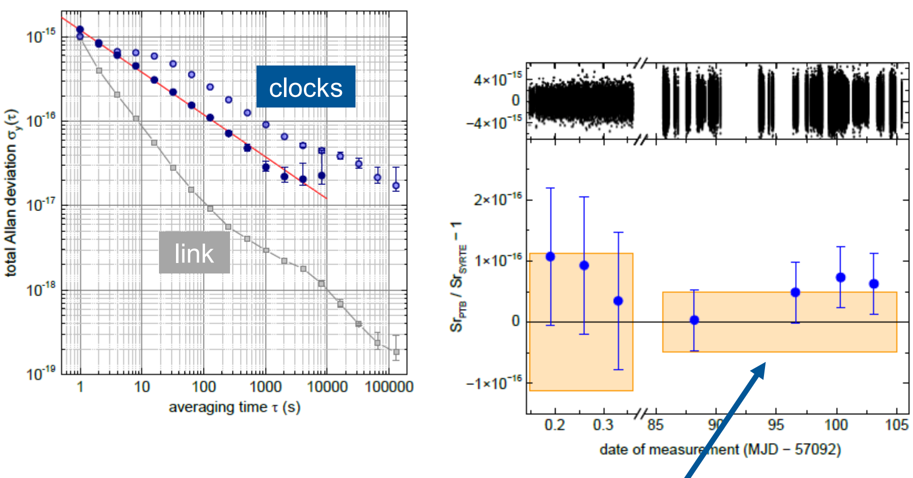

For second campaign, difference = $(4.7 \pm 5.0) \times 10^{-17}$

Lisdat *et al.*,
arXiv: 1511.07735 (2015)

London – Paris optical fibre link

NPL | QMI

- Complete link first operational in June 2015 but signal-to-noise too poor for optical clock comparisons
- Improvements have now been implemented and full loop characterisation is underway

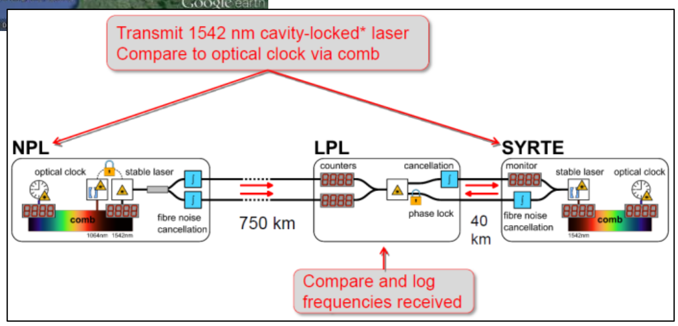

NPL | QMI

Handling over-determined sets of clock comparison data

Secondary representations of the second

- Recommended frequencies and uncertainties are assigned by the Frequency Standards Working Group (WGFS) of the CCTF and CCL
- Values are periodically updated and published at www.bipm.org/en/publications/mises-en-pratique/standard-frequencies.html
- Almost all data considered so far comes from absolute frequency measurements relative to Cs primary standards
- Future information about reproducibility of optical standards will come mainly from direct optical frequency ratio measurements

Over-determined sets of clock comparison data

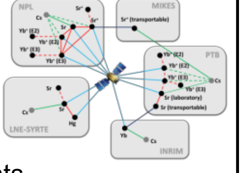

- Within the ITOC project, we will end up with
  - A set of frequency ratio measurements between optical clocks
  - A set of Cs-limited absolute frequency measurements
- It will be possible to deduce some frequency ratios from several different measurements
- For example, ν_{Yb+} / ν_{Sr} could be measured either directly, or indirectly by combining two or more other frequency ratio measurements,
  e.g. $\nu_{Yb+} / \nu_{Sr} = (\nu_{Yb+} / \nu_{Yb})(\nu_{Yb} / \nu_{Sr})$ or $\nu_{Yb+} / \nu_{Sr} = (\nu_{Yb+} / \nu_{Cs})(\nu_{Cs} / \nu_{Sr})$
- Multiple routes to deriving each frequency ratio value mean that it will no longer be possible to treat each optical clock in isolation when considering the available data

Analysis of the frequency ratio matrix

- Aim is to develop methods for analysing all available data from clock comparison experiments
  a) To check the level of internal self-consistency
  b) To derive optimal values for the ratios between their operating frequencies

- Use a least-squares adjustment procedure, based on the approach used by CODATA to provide a self-consistent set of recommended values of the fundamental physical constants
  [Mohr & Taylor, Rev. Mod. Phys. 72, 351 – 495 (2000)]

- All data stored as frequency ratios (optical frequency ratios, microwave frequency ratios or optical-microwave frequency ratios)

H. S. Margolis and P. Gill, Metrologia 52, 628 (2015)

Input data to the least-squares adjustment

- Suppose that the frequency standards involved in the comparison experiments are based on N_S different reference transitions with frequencies ν_k (k = 1, 2, … N_S)

  e.g. ν_1 could be the 5s^2 ^{1}S$_0$ – 5s5p ^{3}P$_0$ transition in ^{87}Sr at 698 nm
  ν_2 the 6s ^{2}S$_{1/2}$ – 4f^{13}6s^2 ^{2}F$_{7/2}$ transition in ^{171}Yb$^+$ at 467 nm
  ν_3 the 6s ^{2}S$_{1/2}$ (F=3) – 6s ^{2}S$_{1/2}$ (F=4) transition in ^{133}Cs at 9.2 GHz
  and so on

- Set of comparison experiments yields a set of N measured quantities q_i of various quantities (frequency ratios)

- Measured values q_i, together with their variances and covariances form the input to the least-squares adjustment

Correlations are included

Least-squares analysis procedure

Set of N measured frequency ratios, variances and covariances

Choose set of $M = N_S - 1$ adjusted frequency ratios

Must satisfy the condition that no adjusted frequency ratio z_j may be expressed as a function of the others,

e.g. $z_1 = \nu_1 / \nu_2$, $z_2 = \nu_2 / \nu_3$, …

These are equivalent to the adjusted constants in the CODATA analysis of the fundamental physical constants.

Least-squares analysis procedure

Set of N measured frequency ratios, variances and covariances

Choose set of $M = N_S - 1$ adjusted frequency ratios

Express measured frequency ratios in terms of adjusted frequency ratios, yielding a set of N equations

$$q_i \doteq f_i(z_1, z_2, \ldots, z_M) \qquad \text{where } i = 1, 2, \ldots, N$$

e.g. q_1 might be ν_2 / ν_5, which can be expressed as $z_2\, z_3\, z_4$

q_2 might be either another measurement of ν_2 / ν_5 or a measurement of a different ratio such as ν_2 / ν_6

Least-squares analysis procedure

- Set of N measured frequency ratios, variances and covariances
- ↓ Choose set of $M = N_S - 1$ adjusted frequency ratios
- ↓ Express measured frequency ratios in terms of adjusted frequency ratios, yielding a set of N equations
- ↓ Linearize equations using Taylor expansion around initial estimates of adjusted ratios ← Initial estimates of adjusted frequency ratios

$$q_i \doteq f_i(s_1, s_2, \ldots, s_M) + \sum_{j=1}^{M} \frac{\partial f_i(s_1, s_2, \ldots, s_M)}{\partial s_j}(z_j - s_j) + \ldots$$

or

$$y_i \doteq \sum_{j=1}^{M} a_{ij} x_j$$

where

$$y_i = q_i - f_i(s_1, s_2, \ldots, s_M)$$

$$x_j = z_j - s_j$$

$$a_{ij} = \frac{\partial f_i(s_1, s_2, \ldots, s_M)}{\partial s_j}$$

Enables linear matrix methods to be applied

Least-squares analysis procedure

- Set of N measured frequency ratios, variances and covariances
- ↓ Choose set of $M = N_S - 1$ adjusted frequency ratios
- ↓ Express measured frequency ratios in terms of adjusted frequency ratios, yielding a set of N equations
- ↓ Linearize equations using Taylor expansion around initial estimates of adjusted ratios ← Initial estimates of adjusted frequency ratios
- ↓ Perform least-squares adjustment
- ↓ Best values of adjusted ratios, variances and covariances

In matrix notation, equations become $\boldsymbol{Y} \doteq \boldsymbol{AX}$

Least-squares adjustment minimises the product

$$S = (\boldsymbol{Y} - \boldsymbol{AX})^T \boldsymbol{V}^{-1} (\boldsymbol{Y} - \boldsymbol{AX})$$

with respect to $\boldsymbol{X}$. Here $\boldsymbol{V}$ is the covariance matrix of the input data.

Solution $\hat{\boldsymbol{X}}$ gives best estimate of adjusted frequency ratios.

Least-squares analysis procedure

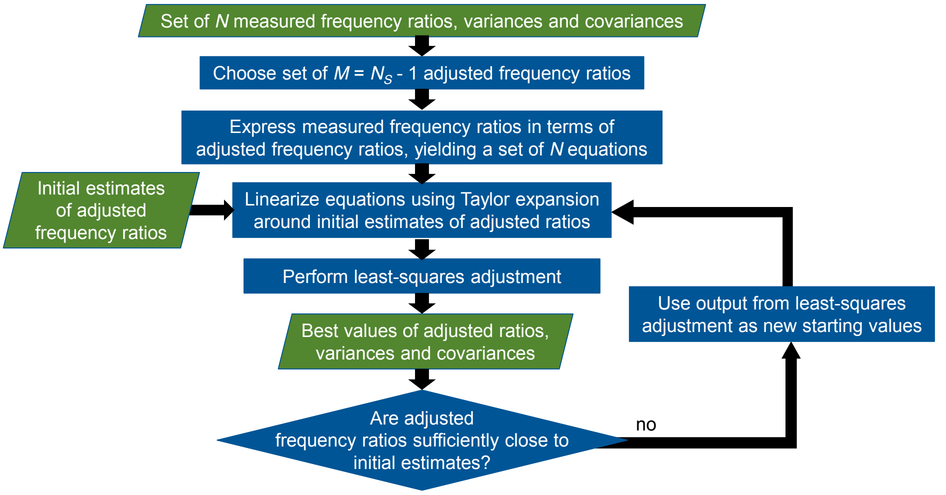

Number of iterations required to achieve convergence depends on how close the initial estimates of the adjusted frequency ratios are to the final values.

Least-squares analysis procedure

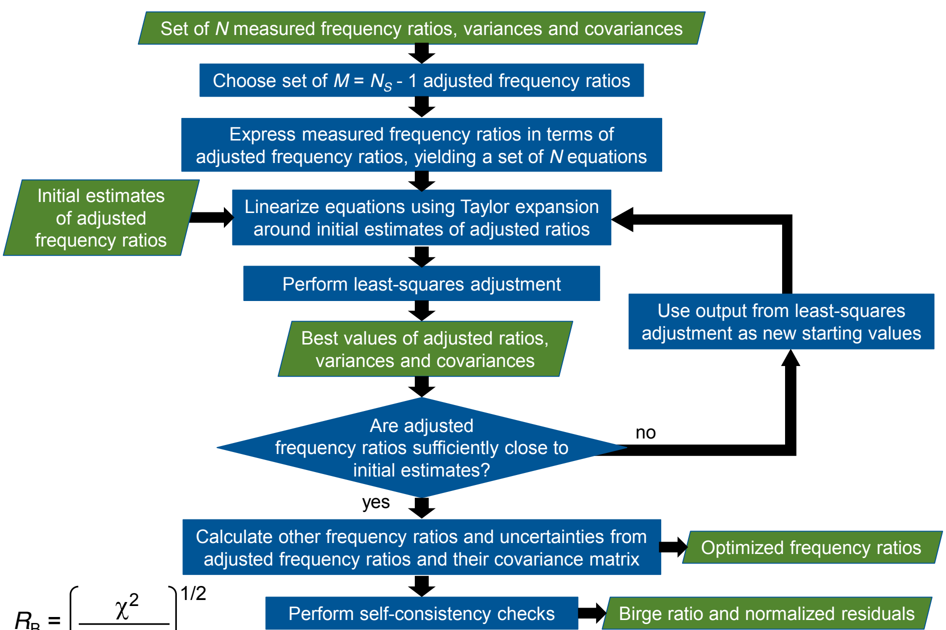

$$R_B = \left(\frac{\chi^2}{N - M} \right)^{1/2}$$

Tests of the software algorithms

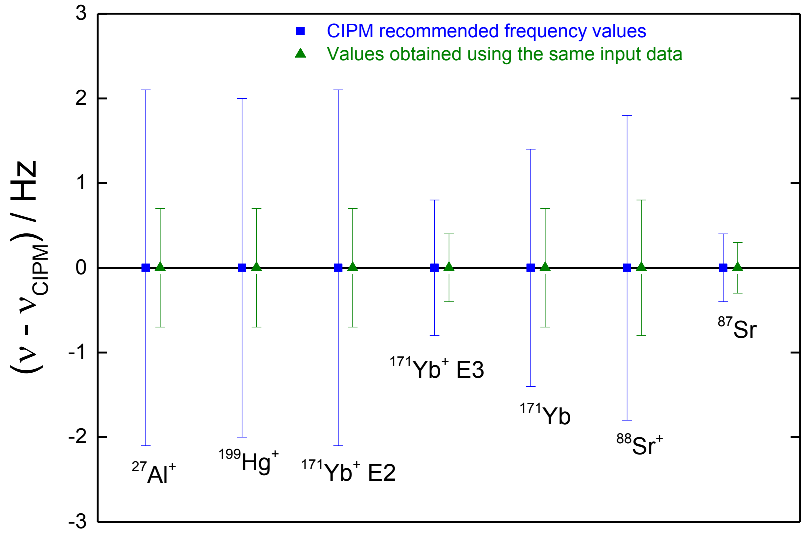

- Reproduces CIPM recommended frequency values
- Uncertainties are smaller, due to conservative approach of WGFS

Inclusion of new clock comparison data

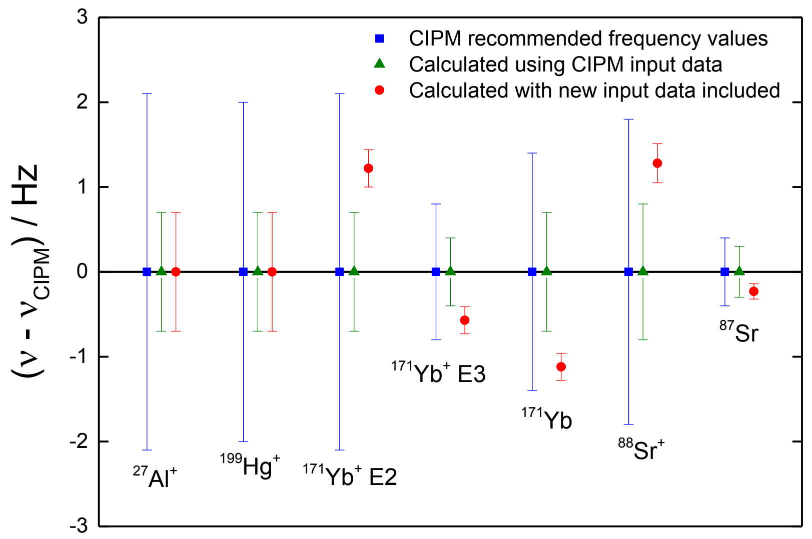

- Significant changes observed for some values
- Conservative approach adopted by the WGFS may be prudent

Importance of correlations

Hypothetical 10-day measurement campaign:

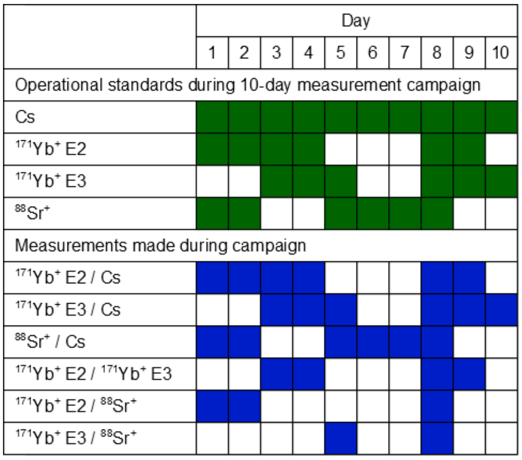

Cs fountain operates 100% of the time

3 optical clocks each operate for 60% of the time, with some periods of overlap

6 different frequency ratios can be determined

12 non-zero correlation coefficients

Correlations arise from both statistical and systematic uncertainties.

Example

- Absolute frequency measurements of $^{171}Yb^+$ E2 transition and $^{88}Sr^+$ transition are correlated because part of the Cs fountain data is common to the two
- Assuming all other sources of uncertainty negligible compared to statistical uncertainty associated with the Cs standard:

  $^{171}Yb^+$ E2 standard runs for a total period T_A = 6 days

  $^{88}Sr^+$ standard runs for a total period T_B = 6 days

  Period of overlap $T_{overlap}$ = 3 days

  Correlation coefficient is $\left(\frac{T_{overlap}^2}{T_A\, T_B}\right)^{1/2} = 0.5$

- In practice, other contributions to uncertainty must also be considered, e.g. systematic uncertainty of Cs fountain is also common to the measurements

Effect of correlations

- Present stabilities and systematic uncertainties of NPL's optical clocks can be used to estimate correlation coefficients for hypothetical measurement campaign
- Values of 12 correlation coefficients range from –0.10 to 0.95
- Largest correlation coefficient is for the $^{171}Yb^+$ E2 / $^{171}Yb^+$ E3 and $^{171}Yb^+$ E2 / $^{88}Sr^+$ frequency ratios (dominated by the systematic uncertainty of the $^{171}Yb^+$ E2 standard)
- For arbitrarily-selected values of the measured frequency ratios resulting from this hypothetical measurement campaign, effect of correlations can be determined

Effect of correlations

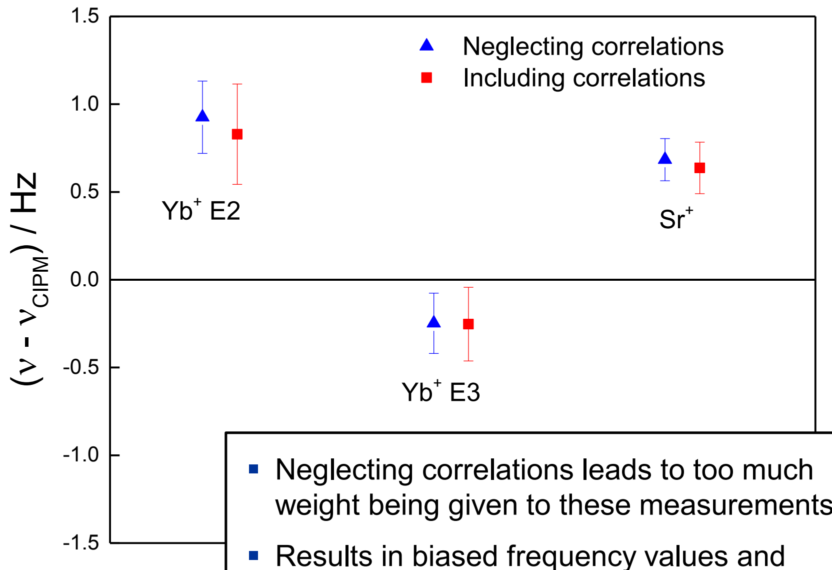

- Neglecting correlations leads to too much weight being given to these measurements
- Results in biased frequency values and underestimated uncertainties

Application of the analysis methods

- Can be used to determine a self-consistent set of frequency ratios between high accuracy standards, based on all available experimental data and including correlations among the data
- As number of direct optical frequency ratio measurements increases, could be used
  - To provide valuable information about relative performance of different candidates for an optical redefinition of the SI second
  - To determine optimized values and uncertainties for absolute frequencies of each optical standard relative to the current definition of the SI second (special cases of frequency ratios)
- Optimized values and uncertainties are required to maximise the potential contribution of optical clocks to international timescales prior to any redefinition

Key issues

- All possible input data must be identified and critically reviewed, especially the standard uncertainty of each measurement
- Correlations between the input data must be considered
  - Information reported in the literature is in many cases insufficient to calculate the correlation coefficients
  - Additional information will be required
- Must investigate
  - Effect to which each input datum contributes to the determination of the adjusted frequency values
  - Effects of omitting inconsistent or inconsequential data
- Issues are common to those faced by the CODATA Task Group on Fundamental Constants
- Likely to be highly relevant to future discussions within the FSWG

Optical clocks, relativity and geodesy

Gravity potential for optical clock comparisons

Geodesy expertise provided by Leibniz Universität Hannover
(Heiner Denker, Ludger Timmen, Christian Voigt)

- Design of setups to determine the static gravity potential at all clock locations
  - Potential differences for clock comparisons
  - Absolute potential values for timescales
- Development of a refined European geoid model including gravity observations around all relevant clock sites
  - Measurement campaigns completed at INRIM, NPL, OBSPARIS, PTB and LSM
- Investigation of time-variable components of the gravity potential, e.g. due to tides

Recommendations for GPS / levelling

NPL National Physical Laboratory | QMI Quantum Metrology Institute

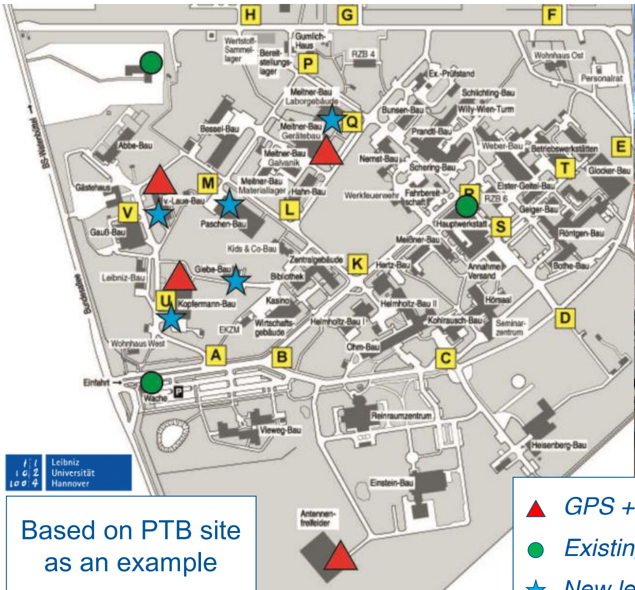

Based on PTB site as an example

- ▲ *GPS + levelling BMs (4)*
- ● *Existing levelling BMs (3, DHHN92)*
- ★ *New levelling BMs (≈20)*

Gravity measurements (INRIM)

NPL National Physical Laboratory | QMI Quantum Metrology Institute

Campaign in September 2013

- One absolute gravity measurement
- 35 relative gravity measurements

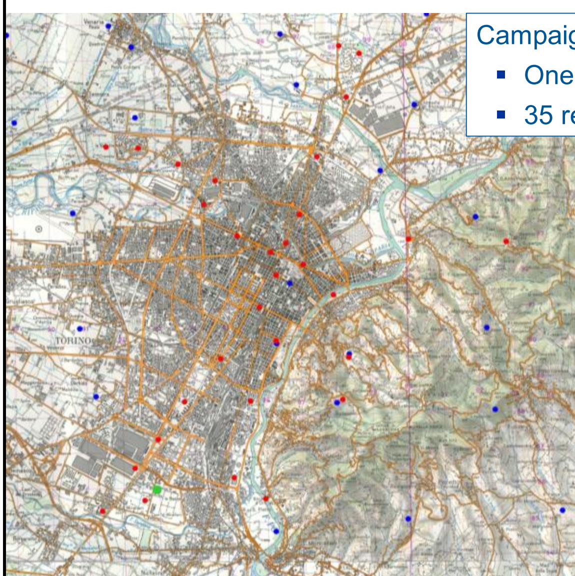

Gravity measurements (NPL)

Campaign in March 2014

- 2 absolute gravity measurements
- 64 relative gravity measurements

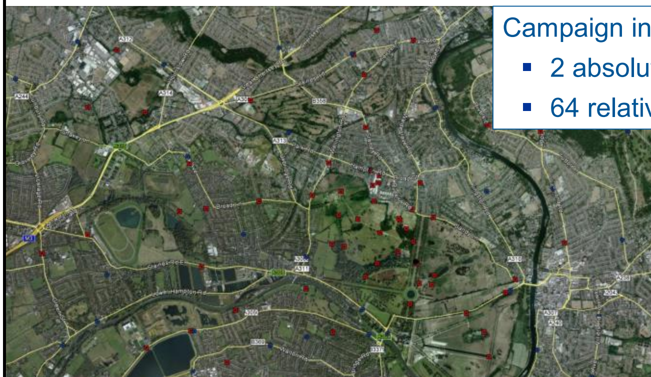

Gravity measurements (OBSPARIS)

Campaign in October 2014

- 3 absolute gravity measurements
- 99 relative gravity measurements

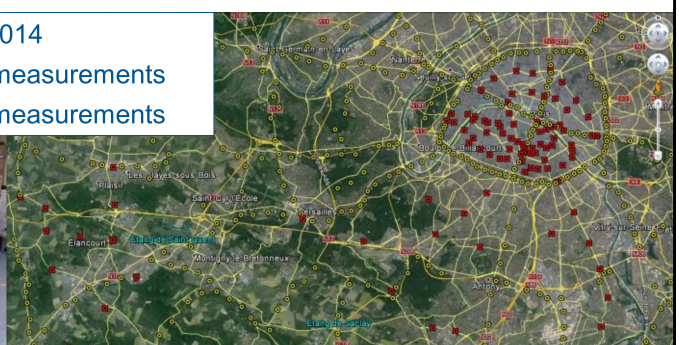

Gravity measurements (PTB)

Campaigns in March & October 2014

- 1 absolute gravity measurement
- 83 relative gravity measurements

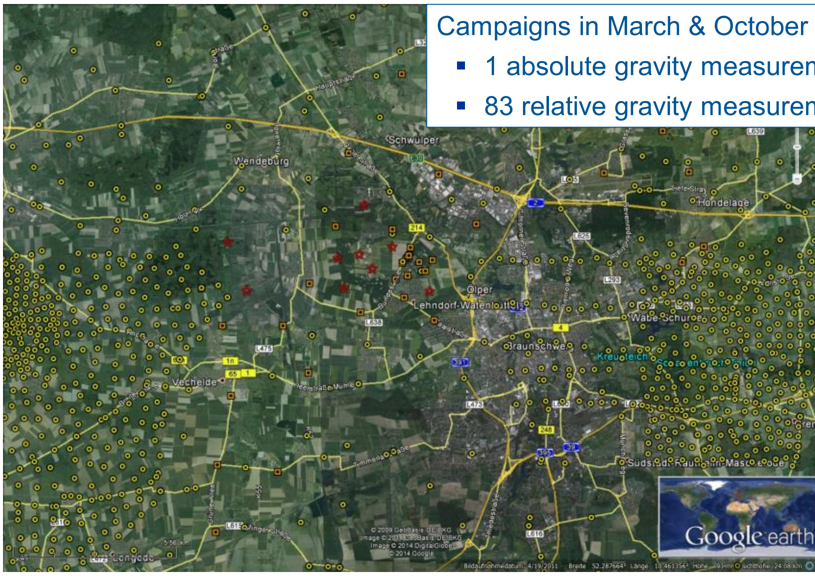

European Gravimetric (Quasi)Geoid 2015 (EGG 2015)

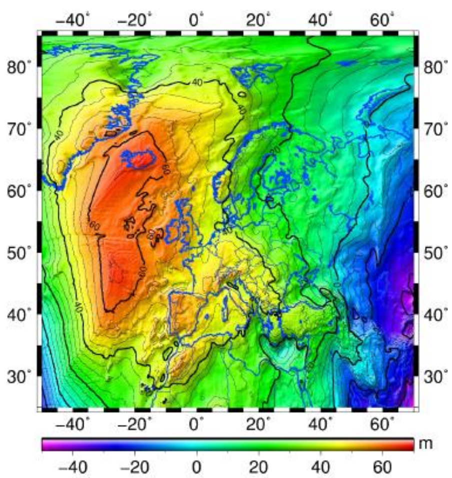

- Long wavelength components computed from a global Earth gravity model
- Short wavelength components computed from high resolution digital elevation models
- Medium wavelength structures recovered from terrestrial gravity data

Accuracy ~ few cm

Clock-based geodesy

Direct measurement of the earth’s gravity potential with high resolution by using the gravitational redshift.

Frequency shift $$Z \equiv \frac{\Delta f}{f} = \frac{\Delta U}{c^2}$$

ΔU = gravity potential difference between clocks

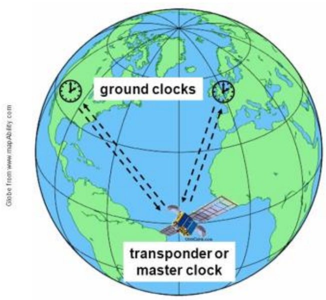

Comparison of terrestrial clocks with 10^{-18} accuracy

↓

Measurement of gravity potential differences with equivalent height resolution of 1 cm

Proof-of-principle clock-based geodesy experiment

Aim: To show that optical clocks can be used to measure gravity potential differences over medium – long baselines with high temporal resolution

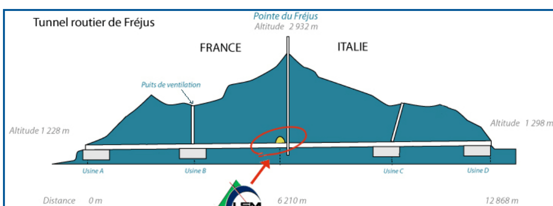

ITOC consortium

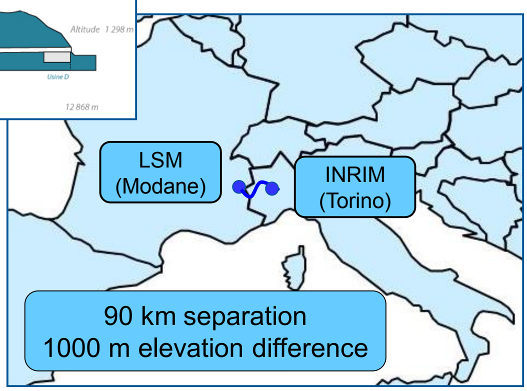

Proof-of-principle clock-based geodesy experiment

Proof-of-principle clock-based geodesy experiment

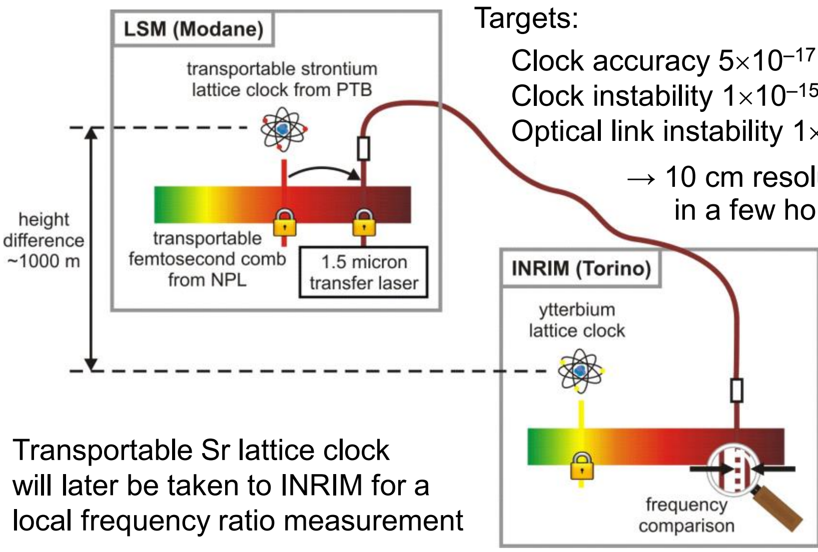

Gravitational redshift ~ 10^{-13}

Targets:

- Clock accuracy 5×10^{-17}
- Clock instability $1\times10^{-15}\,\tau^{-1/2}$
- Optical link instability $1\times10^{-14}\,\tau^{-1}$

$\rightarrow$ 10 cm resolution in a few hours

Transportable Sr lattice clock will later be taken to INRIM for a local frequency ratio measurement

Experiment in progress now…

Sr lattice clock

clock laser

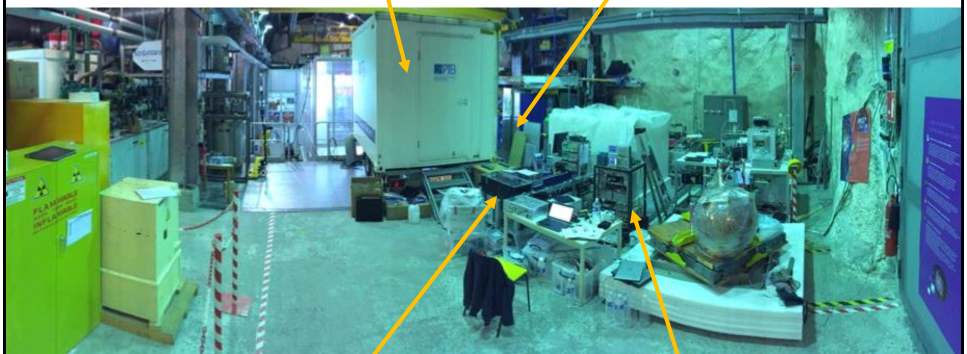

frequency comb

fibre link from INRIM

All 6.5 km inside the Fréjus tunnel…

Gravity measurements (LSM)

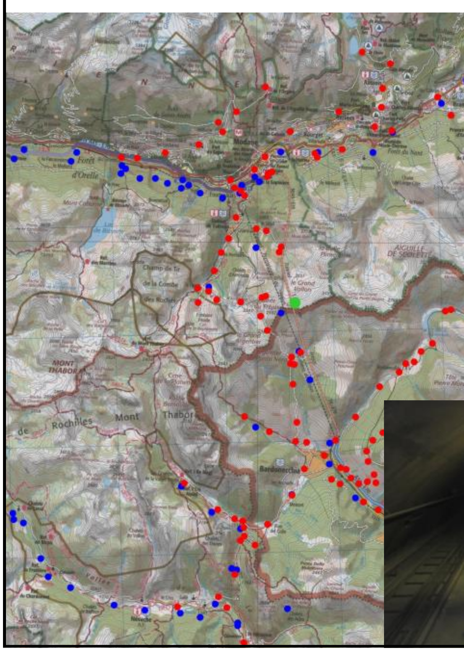

Campaign in September 2013

- One absolute gravity measurement
- 122 relative gravity measurements

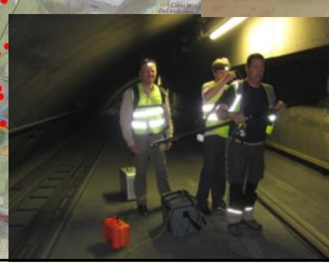

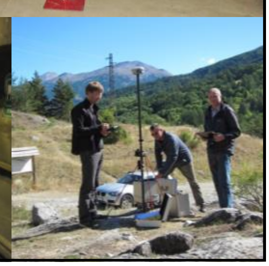

Fundamental physics with optical clocks

Tests of fundamental physics

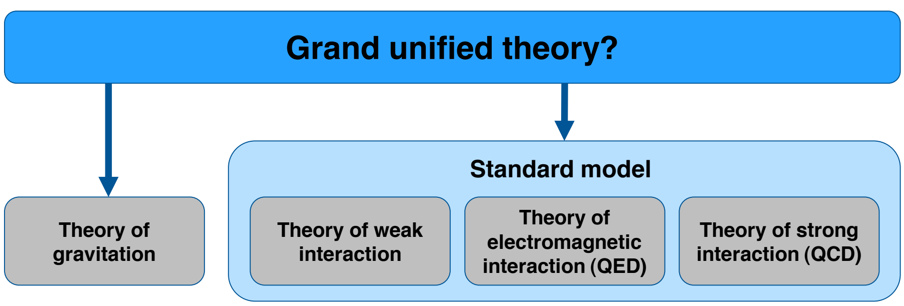

- General relativity is fundamentally incomplete –
  violations of underlying principles are expected
- Theoretical attempts to unify gravity with the electroweak and strong interactions predict violations of the Einstein Equivalence Principle
- Effects small and challenging to measure with high precision

Do fundamental constants vary with time?

If local position invariance holds, then fundamental physical constants should be constant in time.

Any optical transition frequency can be written as $F = C\,F(\alpha)\,R_\infty c$

Rate of change with time is $\frac{\partial}{\partial t}\ln f = A\frac{\partial}{\partial t}\ln\alpha + \frac{\partial}{\partial t}\ln(R_\infty c)$

Ion	Clock transition	*A*
Sr^+	$^2S_{1/2} - {}^2D_{5/2}$	0.43
Yb^+	$^2S_{1/2} - {}^2D_{3/2}$	0.88
Yb^+	$^2S_{1/2} - {}^2F_{7/2}$	-5.95
Hg^+	$^2S_{1/2} - {}^2D_{5/2}$	-2.94
In^+	$^1S_0 - {}^3P_0$	0.18
Al^+	$^1S_0 - {}^3P_0$	0.008

where $A = \frac{\partial \ln F(\alpha)}{\partial \ln \alpha}$

Frequency ratios between dissimilar optical clocks depend on the fine structure constant α.

Dzuba *et al.*, Phys. Rev. A 59, 230 (1999)
Angstmann *et al.*, Phys. Rev. A 70, 014102 (2004)
Dzuba *et al.*, Phys. Rev. A 68, 022506 (2003)
Dzuba et al, Phys. Rev. A 77, 012515 (2008)

Laboratory tests

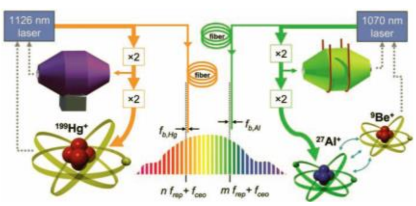

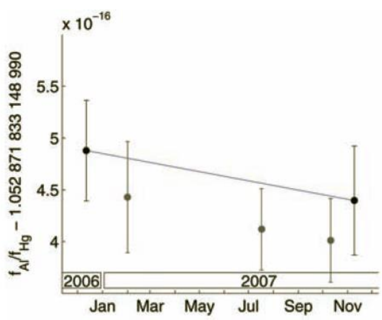

Comparison between $^{199}Hg^+$ and $^{27}Al^+$ optical clocks at NIST:

$$\frac{f_{Al+}}{f_{Hg+}} = 1.052\,871\,833\,148\,990\,438\,(55)$$

Relative uncertainty 5.2 x 10^{-17}

- 4.3 x 10^{-17} statistics
- 1.9 x 10^{-17} Hg^+ systematics
- 2.3 x 10^{-17} Al^+ systematics

Repeated measurements over 1 year:

$$\frac{\dot{\alpha}}{\alpha} = (-1.6 \pm 2.3) \times 10^{-17}\ /\ \text{year}$$

Rosenband *et al.*, Science 319, 1808 (2008)

Frequency ratio measurements in $^{171}Yb^+$

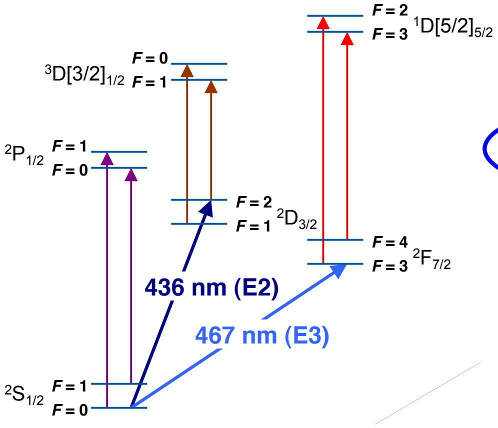

Ion	Clock transition	*A*
Sr^+	$^2S_{1/2} - {}^2D_{5/2}$	0.43
Yb^+	$^2S_{1/2} - {}^2D_{3/2}$	0.88
Yb^+	$^2S_{1/2} - {}^2F_{7/2}$	-5.95
Hg^+	$^2S_{1/2} - {}^2D_{5/2}$	-2.94
In^+	$^1S_0 - {}^3P_0$	0.18
Al^+	$^1S_0 - {}^3P_0$	0.008

$$\frac{\dot{r}}{r} = 6.83\,\frac{\dot{\alpha}}{\alpha}$$

Interleaved interrogation of two optical clock transitions in the same ion in the same environment

➡ common-mode rejection / reduction of some (but not all) systematic frequency shifts

S. N. Lea, Rep. Prog. Phys. 70, 1473 (2007)

Recent measurements in $^{171}Yb^+$

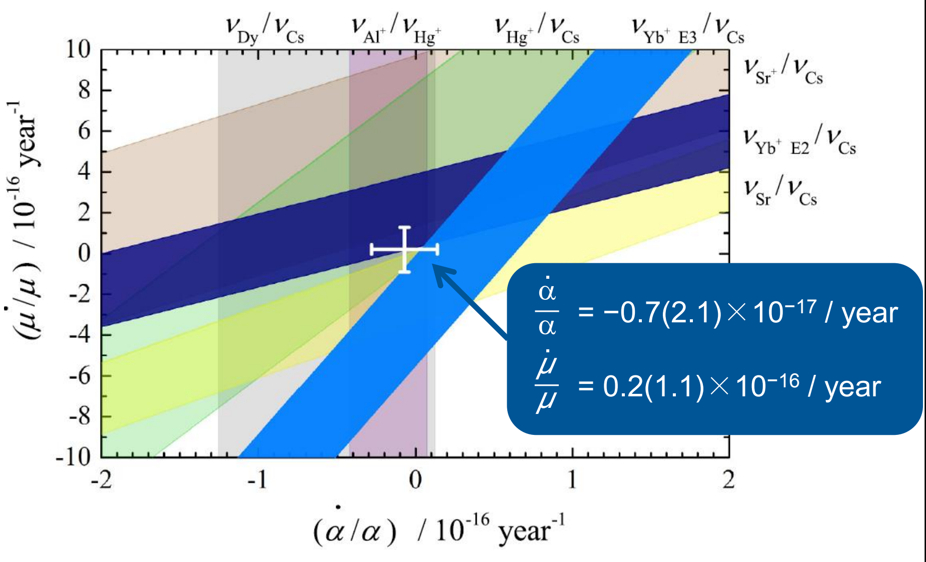

$$\frac{\dot{\alpha}}{\alpha} = -0.7(2.1)\times 10^{-17}\ /\ \text{year}$$

$$\frac{\dot{\mu}}{\mu} = 0.2(1.1)\times 10^{-16}\ /\ \text{year}$$

Godun *et al.*, Phys. Rev. Lett. 113, 210801 (2014)

Similar analysis in Huntemann *et al.*, Phys. Rev. Lett. 113, 210802 (2014)